STUDY ON APPLICATION MODELS OF FRACTIONAL DERIVATIVES

KAUSHIK B JAIN
21MPBS407039

VARUN GOWDA
21MPBS407034

Mentor
Dr. SINDHU J ACHAR

Contents

List of Figures

List of Tables

1 Introduction

It is possible to believe that mathematics plays a minor or nonexistent role in the study of biology. Despite the fact that mathematics and biology are two very distinct sciences, mathematicians and biologists collaborated to create **Mathematical Biology**, which is used in biological, biomedical and biotechnology research for both theoretical and practical purposes. Mathematical biology is now recognized as a area of research in applied mathematics. In this paper we study the role of mathematics in biology.

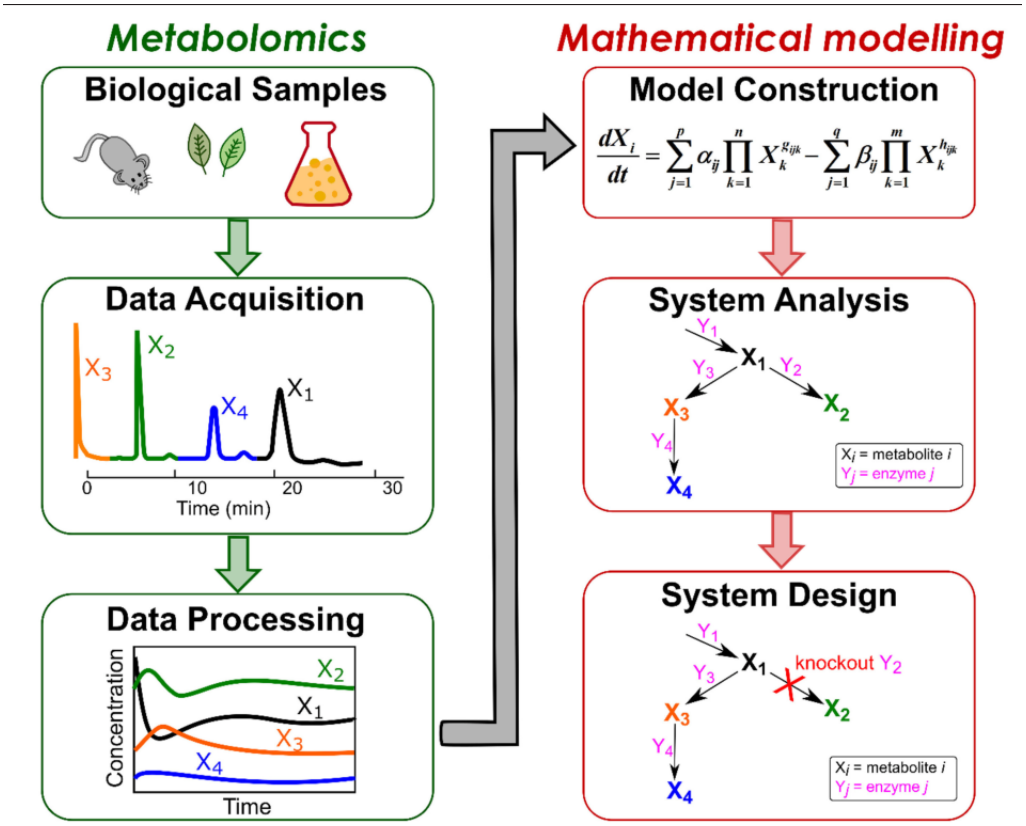

1.1 Mathematical Biology

Currently, Mathematical Biology is a thriving and fascinating field. Fibonacci utilised the well-known Fibonacci series to explain how the number of rabbits was increasing. Daniel Bernoulli used Mathematics in the 18th century to explain how smallpox affected the human population using methods and resources from Applied Mathematics, **Mathematical Biology seeks to represent and simulate Biological processes Mathematically.** It has applications in both theoretical and applied research.

The use of Mathematical Models has been crucial to our comprehension of practically every aspect of Biology. An abstraction of a system's essential elements and procedures is called a model. In order to comprehend the mechanisms that link the system components, we investigate the effects of these connections and forecast how changes in one area of the system affect other areas and then we evaluate these as simplified representations of the world.

A Mathematical Model is a simplified representation of a real-world phenomenon expressed in mathematical language. We develop a model by creating a system of differential equations. The solution of the equations, using analytic or numerical methods, describes how the Biological system acts throughout time or at equilibrium. There are various types of equations and the type of behaviour that can occur is determined by both the model and the equations utilized. The model frequently makes some assumptions about the system and components involved. The equations may also include assumptions about the nature of results.

The goal of theoretical approaches to biological organisation is to comprehend how an organism's components in the system are interdependent. They draw attention to the circularities that result from these interdependencies. A number of ideas were created by theoretical biologists to formalise this notion.

1.1.1 Applications of Mathematical Biology

- Predator Prey models.

- The distribution, metabolism and outflow of drugs and medicines inside the human body are modelled using FDEs.
- To describe neural processes and capture the memory effects seen in the brain's reaction to events.
- The behavior of viscoelastic materials such as gels, polymers and biological tissues are observed.
- To describe particle movement in complex media.
- Mathematical Modelling of scar tissue formation.
- Observation of spread of diseases and Precautionary measures.
- Mathematical Model of Pluviculture.

Ischemic Wounds - A formulated BioMathematical Model [A Case Study] :-

Chronic wounds are wounds that does not heal in an orderly set of stages and in a predictable amount of time. It represents a major public health problem worldwide. Vascular complications are primarily responsible for ischemic wounds(shortage of blood flow). **Ischemic wounds** can occur when there is poor blood flow in your legs. Ischemic wounds is the reduced blood flow to any area of the body. Poor blood flow causes cells to die and damages tissue.

A model was formulated by Xue and Friedman [1] in terms of a system of partial differential equations in a viscoelastic, partially healed domain where a portion of the boundary, namely the open wound's surface, is a free boundary unknown in advance. The Mathematical Model was developed which incorporated the main variables involved in the wound closure phase of the healing process like 'several types of blood and tissue cells', 'chemical signals' and 'tissue density'. The model is shown in the below figure [1.1.1]

$$(1-\alpha)(u-u_s)+\alpha\frac{\partial u}{\partial r}=0 \text{ at r = L}$$

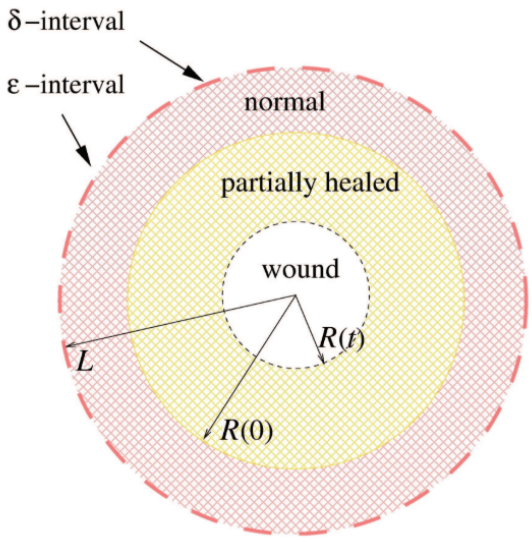

Figure 1: The open wound is the circular region ($0 \leq r \leq R(t)$), the partially healed region is the annulus ($R(t) \leq r \leq R(0)$) and the normal healthy tissue is ($R(0) \leq r \leq L$

.

1.1.2 Literature Review of Mathematical Biology

Ingalls and Brian [2] have introduced about Mathematical models in systems biology. Nagy and John [3] have reviewed about the Ecology and evolutionary Biology of cancer using mathematical models of necrosis and tumor cell. Bakshi et al. [4] have discussed about a Mathematical model of Parkinson's disease . Inan et al. [5] have explained the Analytical and Numerical Solutions of Mathematical Biology models. Nowak et al. [6] have studied about Mathematical Biology of HIV infections

1.2 Predator Prey Model

Models of predator-prey are perhaps the fundamental components of bio-ecosystems, since biomasses develop from their resource masses. In order to find resources to continue their quest for survival, species compete, change, and disperse. They can take on the shapes of resource-consumer, plant-herbivore, parasite-host, tumour cells (virus)-immune system, susceptible-

infectious connections, etc., depending on their particular application conditions. They may find use outside of ecosystems since they address the general loss-win dynamics. Upon close examination, behaviours that appear to be competitive may actually be disguised kinds of predator-prey interactions.

A General Predator-Prey Model:-

Let us examine two populations x(t) and y(t) respectively, representing their sizes at a reference time t. Although they are assumed to be continuous functions, the functions x and y may represent population sizes or some other scaled measure of the populations. The time derivatives $\dot{x} \equiv \frac{dx}{dt}$ and $\dot{y} \equiv \frac{dy}{dt}$ respectively reflect changes in population size with time, and a generic model of interacting populations is expressed in terms of two autonomous differential equations.

$$\dot{x} = xf(x, y)$$

$$\dot{y} = yg(x, y)$$

The time t does not appear explicitly in the functions x $f(x, y)$ and y $g(x, y)$ .The functions f and g denotes per capita growth rates of two species respectively. We assume $\frac{df(x,y)}{dy} < 0$ and $\frac{dg(x,y)}{dx} > 0$. This general model is often called Kolmogorov's predator-prey model

Lotka -Volterra Model :-

A differential equation model was put up in 1926 by the renowned Italian mathematician Vito Volterra to explain the reported rise in predator fish (and concomitant decline in prey fish) in the Adriatic Sea during World War I. Alfred Lotka (1925) independently derived the equations that Volterra researched at the same time to describe a hypothetical chemical reaction in which the chemical concentrations oscillate. The most basic model of interactions between predators and prey is the Lotka-Volterra model. Its foundation is the linear per capita growth rates expressed as

$$f = b - py \quad \text{and}$$

$$g = rx - d$$

- The growth rate of species x (the prey) in the absence of interaction with species y (the predators) is represented by the parameter b. These interactions reduce the number of prey, As x increases, the per capita growth rate falls (linearly) and may turn negative.
- The parameter p is the impact of predation on $\dot{x}/x$.
- The parameter d is the death rate of species y in the absence of interaction with species x .
- The term rx denotes the net rate of growth of the predator population in response to the size of the prey population.

The Prey-Predator model with linear per capita growth rate is

$$\dot{x} = (b - py)x \text{ (Prey)}$$
$$\dot{y} = (rx - d)y \text{ (predator)}$$

This system of equations is referred to the Lotka-Volterra model

1.2.1 Functional Response and its types

The relationship between the density of prey and the predator's per capita consumption is explained by the functional response. Numerous functional and numerical reactions have been identified by different Holling Types

- **Holling type-I :-**

  The type I functional response linearly increases intake rate with food density, either for all food densities or up to a mark, after which the intake rate is constant. The linear growth model makes assumptions that eating does not impede one's ability to search for food, or that the time a consumer needs to process a food item is negligible. The Lotka-Volterra predator-prey model is a functional response of Holling type I. [1.2.1]

$$f(x) = ax,\ 0 < x < a$$
$$f(x) = \gamma,\ a \leq \gamma$$

Where, a is the value of prey density at which the predator satiate and γ is the constant rate of predation after satiation.

- **Holling type-II (Cycloid) :-**

  The type II functional response is poised by decreasing intake rate, we understand that the consumer's capacity to metabolize food is limited. Frequently, a rectangular hyperbola, such as Holling's disc equation, which concludes that food processing and food finding are mutually incompatible actions. [1.2.1]

$$f(R) = \frac{aR}{1 + ahR}$$

  f signifies the rate of consumption
  R the density of food
  a is the Attack rate
  h is Handling Time

- **Holling type-III (Sigmoid) :-**

  The type III functional response has similarities with type II. At high levels of prey density, saturation occurs and at low prey density levels, a hyper linearly increasing function of the amount of prey consumed by predators may be seen in the graphical relationship between the number of preys consumed and the density of the prey population. [1.2.1]

$$f(x) = \frac{aR^k}{1+ahR^k} \ , \ k > 0$$

  For k = 2, this accelerating function was originally defined in terms of the kinetics of an enzyme with two binding sites.

- **Holling type-IV :-**

  This kind of interaction is denoted by,

$$f(x) = \frac{ax}{(\frac{x^2}{a}+x+\eta)} \ \ , \ a, b > 0$$

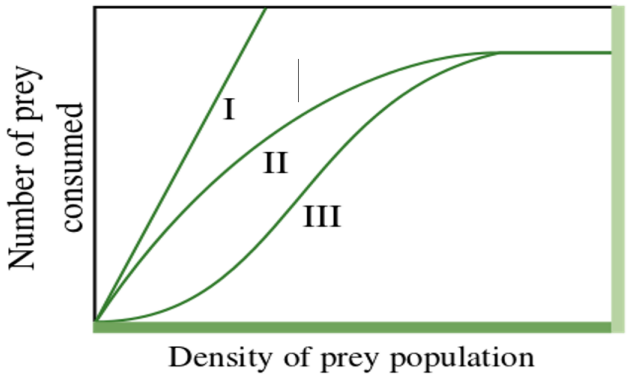

Figure 2: Holling Types Graph

.

- **Ratio-Dependent Functional Response :-**

  Here, the terms are expressed based on the ratio of the prey to their respective predators and named it as a ratio-dependent functional response. It is given by,

$$f(x, y) = \frac{\delta y}{ax + by}$$

  Beddington and DeAngelis have formulated a new general ratio-dependent functional response. It is given by

$$f(x, y) = \frac{\delta y}{a + bx + cy}$$

  Here, δ, a, b, c are constants. The above functional response is termed as Beddington-DeAngelis functional response which is very similar to Holling type-II response except the extra term cy in the denominator which describes the mutual interference between the predators.

1.3 Types of Predator Prey Models

1.3.1 Epidemiological Model

An abnormally large, brief breakout of a disease is called an epidemic. An illness is deemed endemic if it continues to exist within a community. In addition to disease-related elements including the infectious agent, method of

transmission, latent period, infectious period, susceptibility, and resistance, social, cultural, demographic, economic, and geographic factors also have a role in the spread of infectious diseases.

Epidemic modeling describes a set of approaches where mathematical, statistical, and computational tools are used to study the spread of communicable pathogens in host populations. It uses data and theories to explain how environmental characteristics, illness impacts on health, chances for transmission, and demographic processes work. Equipped with the right evolution-related equations, it can be used for quantification, hypothesis-based forecasting and scenario creation, and logical verification through conceptual experiments.It makes use of information and theories to explain the health effects of diseases, environmental traits, transmission opportunities, and demographic processes. Equipped with appropriate equations for evolution, it can be applied to quantification, logical verification via conceptual experiments, and hypothesis based on forecasting and scenario design. In simple words, **Epidemiological models are mathematical representations of infectious disease outbreaks to understand the course of disease evolution in a population.**

Similar to other scientific fields, these models concentrate on the subset of characteristics and functionswhich are crucial drivers in order to provide a close condensed picture of actual phenomena. Therefore, the structural decisions made in the creation of these models are considered by previous research, data and observations as well as a set of presumptions are made by looking at the model process and components.

Many modeling approaches are used in epidemiology today, building on decades of progress at the intersection of biology, medicine, and demography. The vast majority of models describe the illness as a process from infection to recovery or death, using a compartmentalized approach. The **S-I-R model**, which describes people vulnerable to Susceptible (S), then Infected with the disease (I), and ultimately eliminated from transmission by Recovery (R) [Figure 1.3.1]. The non-linear equation for the evolution of disease results from incidence spread, in such models both are proportional to the number of susceptible individuals and the number of infected individuals.

Partial and Fractional Differential equations both can be used to solve

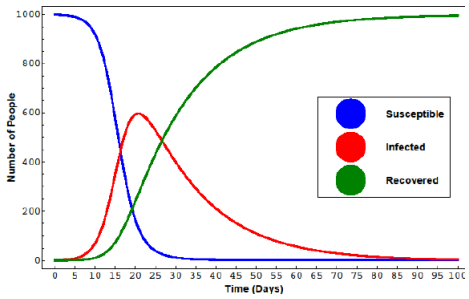

Figure 3: The progression of a epidemic model

these models. Many theoretical and numerical instruments have been developed using this method. This covers, for instance, how to determine the reproduction number in relation to the model's other parameters. It is also incredibly flexible, enabling the natural history to be refined with several stages and the population to be divided based on many attributes (such as age, sex, area, etc.). Stochastic effects can also be taken into consideration while solving the same models, for instance when there is a lot of inter-individual variability and one wants to measure how this heterogeneity affects epidemiologic dynamics.

Significance of Epidemiological Models :-
Despite the fact that many infectious diseases have vaccines available, these illnesses nevertheless inflict pain and death worldwide, particularly in developing nations. Worldwide, infectious diseases continue to be a leading cause of death. The Human Immunodeficiency Virus (HIV) leads to Acquired Immunodeficiency Syndrome (AIDS) has become an important infectious disease in both developing and affluent countries.

For almost all infectious diseases, the method of transmission from susceptibles to infected is understood and the spread of diseases through a chain of infections is well-established. Without the systematic framework of a Mathematical Model, it will be a challenge to understand the large-scale dynamics of the disease spread due to the complexity of the transmission exposition in a population. Even a microscopic description has to be used by an epidemiological model to forecast the macroscopic behaviour of the disease transmission within the analysed community. These models comprehends the complex behaviour of epidemic pathways and possibilities.

Basic Epidemic Models

SIR Epidemic Model :-

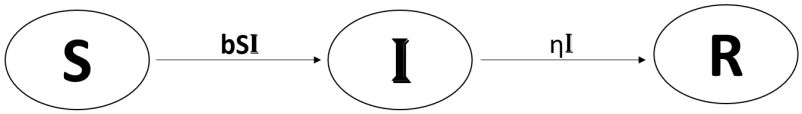

Figure 4: The SIR Model

SIRS Model :-

In this type, the individuals who have retrieved their health last for sometime only on the temporary basis. After losing the immunity, the recovery population again enters the susceptible class. The mean immunity period is given by $\frac{1}{\rho}$. "Immune for the disease is represented by ρR(t) at any time t."

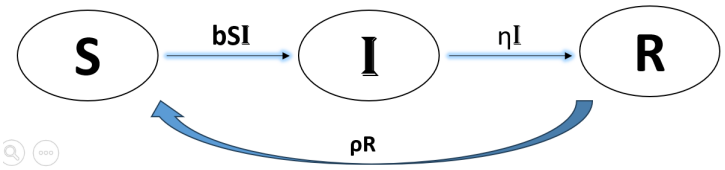

Figure 5: The SIRS Model

SEIS Model :-

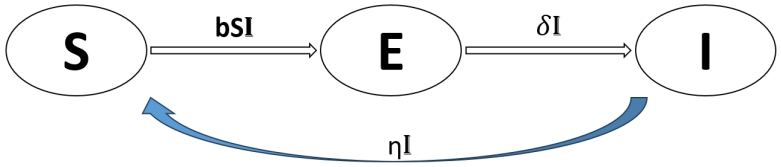

Figure 6: The SEIS Model

SEIR Model :-

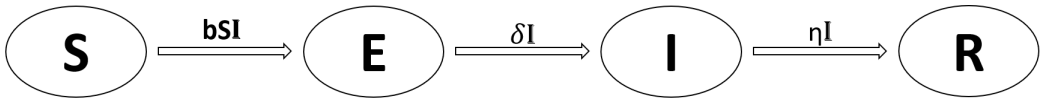

Figure 7: The SEIR Model

In the above models,
S is the Susceptible population
I is the Infected Population
R is the Recovered Population
E is the Exposed Population
b is the disease transmission rate
η is the recovery rate
ρ is the progression rate coefficient of the individuals from recovered to susceptible class
δ is the progression rate coefficient of the individuals from exposed class to infected class and $\frac{1}{\delta}$ is the mean latent period.

1.3.2 Ecological Model

An **Ecosystem** is an interconnected group of living organisms like plants, animals and humans. It also includes their interaction with the nonliving environment elements like water, sunlight and soil. **Ecological models are mathematical representations of ecological systems that are used to understand and predict how different components of an ecosystem interact with each other**. These models can range from simple conceptual models to complex computer simulations that incorporate a wide range of variables and interactions..Constructing and analyzing these mathematical models is known as ecological modeling. This can cover purely biological models as well as those combining biological and physical aspects.Such models might be based on analysis or simulation techniques. They serve to shed light on intricate ecological processes and offer predictions about potential changes in real ecosystems.Public health sector has made extensive use of these ecological models. These models target modifications in personal behaviors while considering the impact of social, physical, and political environments.The concepts for these models are borrowed from biology and applied

to change behavior patterns.

Ecological models are adaptable and depend on the situation. They aid in considering major aspects like personal, social, or environmental factors. But to figure out which specific elements are affecting faculty behavior, local research is needed. In the field of biological ecology, we recognize interactions between individuals of the same species within a population, with other living species in communities and with nonliving physical elements in an ecosystem.

The most commonly used ecology model is the **Socio-Ecological model**. This model takes into account the individual and their connections to other people, organizations, and the entire community to work effectively. This model consists of five levels: Individual, Interpersonal, Organizational, Community, and Public Policy. These stages are depicted in the illustrated figure.[Figure 1.3.2]

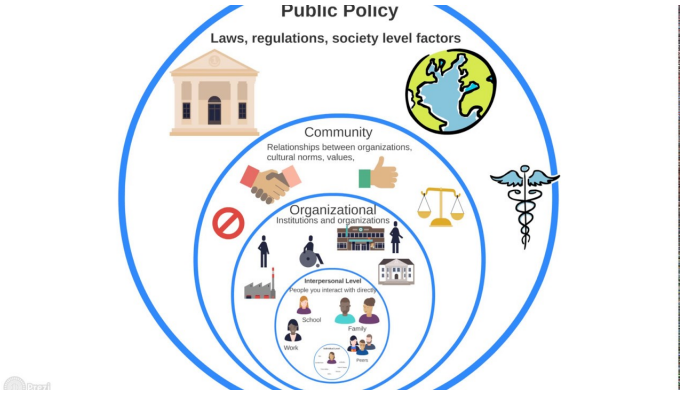

Figure 8: Socio-Ecological Model

Various types of ecological models exist. Some represent the links within an ecosystem, acting as guides. Others mirror the environment, allowing scientists to create digital copies of nature to explore potential changes over time. Once these models are developed, they are utilized for forecasting. For instance, the impact of altering an ecosystem such as tree felling on its animal inhabitants can be predicted using these models. They aid in nature preservation, enable scientists and decision-makers to make informed choices about conservation and natural resource management.

Some real world examples:

The CDC **Colorectal Cancer Control Program (CRCCP)** was created to use elements of an ecological model to address several aspects that influence the prevention of colorectal cancer.

Strong African American Families – TEEN (SAAF-T) used an ecological model to design a family-centered, group-level health promotion and disease prevention program to reduce unprotected sex among adolescents. The program offers health information sessions for adolescents and sessions for their caregivers on communication about risk behaviors.

Significance of Ecological Models :-

The ecological perspective is a practical tool that can help us understand different factors influencing health and well-being. This model sheds light on particular health behaviors, including the social determinants of health. Therefore, we can use ecological models to pull together elements from different theories and models enhancing the creation of thorough health promotion or disease prevention programs or policies. These models are frequently used to evaluate how climate change affects productivity, carbon storage, and resistance to disruptions. They also offer valuable data for creating adaptive strategies for forests.

1.3.3 Literature Review of Epidemiological and Ecological Models

Epidemiological Model Literature Reference :-

Rodrigues and Sofia [7] have discussed about the applications of SIR epidemiological models. Dever and Alan [8] have discussed a case study of an Epidemiological Model for health policy analysis. Martcheva and Maia [9] have introduced us to Mathematical Epidemiology in detail . The [10] have explained us the significance about Epidemiological Models and their use in daily life. Daley et al. [11] have studied on some of very significant Epidemic models.

Ecological Model Literature Reference :-

The [12] have studied about Bio-Ecological theory and their contribution in human development. The [13] discussed multiple levels of influence on health behaviors by Ecological models and some examples.Schuwirth et al. [14] have discussed about the signifcance of Ecological Models. Jackson et al. [15] have

reviewed on the some practices of the Ecological Models. Sallis et al. [16] have given us a insight on various Ecological models of health behavior.

2 Fractional Differential Equations(FDE)

2.1 Introduction

Fractional calculus originated in 1695, when Leibniz and L'Hospital talked about the possibility of taking into account a derivative of order 1/2. This impressed several mathematicians like Laplace, Euler, Letnikov, Grunwald, Riemann, Liouville and so on. **Fractional differential equations (FDEs) gives fractional orders of differentiation**. Applications of these equations can be found in many disciplines, including as biology, engineering, physics, and finance. Fractional calculus, which studies derivatives and integrals of non-integer order, must be studied in order to comprehend FDEs.

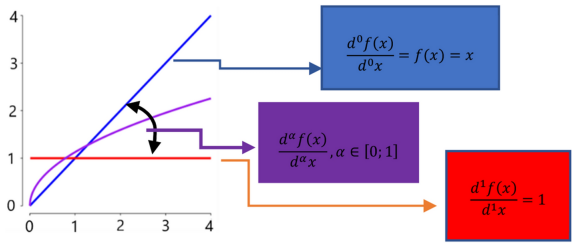

Fractional Derivative

When the order of differentiation is a whole number, traditional calculus works with differentials of integer order. For instance, the acceleration is represented by the second derivative, the rate of change by the first derivative, and so on. Fractional-order derivatives, however, provide a more accurate description of the behaviour in some phenomena, such as anomalous diffusion, viscoelastic materials, and fractal occurrences.

Numerous approaches, such as numerical techniques like finite difference, finite element, and spectral methods, are available for solving FDEs. In some circumstances, analytical techniques like Laplace transforms and series solutions can also be used. When describing phenomena with memory effects and non-local behaviours, fractional differential equations offer a potent framework. Proficiency in fractional calculus and a range of numerical and analytical approaches are necessary for comprehending and resolving FDEs. Their wide range of uses makes them an invaluable instrument for both engineering and scientific research.

2.1.1 Types of Fractional Derivatives and Integrals

- **Caputo fractional derivative :-**

  Suppose that g(t) is k times continuously differentiable function, and $g^{(k)}(t)$ is integrable in $[t_0$,t] . For a function g(t), the fractional derivative of the order α established by the Caputo sense is

$$^{C}D_t^{\alpha} g(t) = \frac{1}{\Gamma(\alpha - k)} \int_{t_0}^{t} \frac{g^{(k)}(S)}{(t-S)^{\alpha+1-k}} ds, \quad k-1 < \alpha < k$$

  Where, $\Gamma(.)$ refers to Gamma function, $t > a$, and k is a positive integer such that, $k-1 < \alpha < k$.

- **Atangana-Baleanu fractional derivative :-**

  Let $g \in H'(a,b), b < a, \alpha \in (0,1]$ be a function. Then, the Atangana-Baleanu fractional derivative of g of order α in Caputo sense is defined at a point $t \in$ (a,b) as,

$$^{ABC}_{a}D_t^{\alpha} g(t) = \frac{B(\alpha)}{1-\alpha} \int_{a}^{t} g'(x) E_{\alpha}(-\alpha \frac{(t-x)^{\alpha}}{1-\alpha}) dx, \alpha \in (0,1], t \in (a,b) \tag{1}$$

  Here E_α refers to Mittag-Leffler function

- **Riemann-Liouville fractional derivative :-**

  Riemann-Liouville fractional derivative is defined by,

$$^{RL}_{a}D_t^{\alpha} g(t) = \frac{1}{\Gamma(k-\alpha)} \left(\frac{d}{dt}\right)^{k} \int_{a}^{t} (t-\tau)^{k-\alpha-1} g(\tau) d\tau, \quad k-1 \leq \alpha < k$$

  The Riemann-Liouville fractional derivative of the power function $g(t) = (t-a)^{\gamma}$ is defined by,

$$^{RL}_{a}D_t^{\alpha} (t-\alpha)^{\gamma} = \frac{\Gamma(\gamma+1)}{\Gamma(-\alpha+\gamma+1)} (t-\alpha)^{\gamma-\alpha} \quad , \quad \gamma > -1$$

- **Grünwald-Letnikov Fractional Derivative (GLFD) :-**

Lets $\alpha > 0$ the Grünwald-Letnikov αth order fractional derivative of function f(t) with respect to t and the terminal value α is given by

$$ {}^{GL}_{a}D^{\alpha}_{t} f(x) = \lim_{h \to 0} h^{-\alpha} \sum_{k=0}^{n} (-1)^{k} \binom{\alpha}{k} f(x - kh) $$

nh= x – a where

$$ \binom{\alpha}{k} = \frac{\alpha(\alpha-1)(\alpha-2)\cdots\cdots(\alpha-k+1)}{k!} = \frac{\Gamma(\alpha+1)}{k!\,\Gamma(\alpha-k+1)} $$

- **Atangana-Baleanu fractional integral :-**

  Atangana-Baleanu fractional integral of order α with base point 'a' is defined as,

$$ {}^{AB}_{a}J^{\alpha}_{t} g(t) = \frac{1-\alpha}{\mathrm{B}(\alpha)} g(t) + \frac{\alpha}{\mathrm{B}(\alpha)\Gamma(\alpha)} \int_{a}^{t} g(x) \ (t-x)^{\alpha-1} \ dx $$

  The Laplace transform associated to Atangana-Baleanu operator is defined as,

$$ L[\,{}^{AB}_{a}J^{\alpha}_{t} g(t)] = \frac{B(\alpha)}{1-\alpha} \frac{s^{\alpha} L(g(t)) - s^{\alpha-1} g(t_0)}{s^{\alpha} + \frac{\alpha}{1-\alpha}} $$

- **Riemann-Liouville fractional integral :-**

  The Riemann-Liouville fractional order integral operator is defined by,

$$ J^{\alpha}_{x} f(x) = \frac{1}{\Gamma(\alpha)} \int_{0}^{x} \frac{f(t)}{(x-t)^{\alpha-1}} dt, \ \alpha > 0 $$

$$ J^{0} g(x) = g(x) $$

  For Riemann-Liouville fractional order integral operator, we have

$$ J^{\alpha}_{x} x^{\gamma} = \frac{\Gamma(\gamma+1)}{\Gamma(\gamma+1+\alpha)} x^{\gamma+\alpha} $$

2.1.2 Advantages of Fractional Differential Equations

Fractional differential equations (FDEs) are an effective mathematical tool that incorporate fractional orders into the concept of differentiation, expanding it beyond integer orders. FDEs provide a more sophisticated and adaptable framework for simulating intricate processes with memory, non-locality, and long-range interactions than classical differential equations, which regulate phenomena with integer-order derivatives. We will now examine the benefits of fractional differential equations in a number of scientific and engineering domains.

- **Modelling Complex Systems :-**

  Fractional-order behaviour is exhibited by many natural phenomena, including anomalous diffusion, viscoelasticity, and fractional-order dynamics in biological systems.

- **Flexibility and Versatility :-**

  FDEs are capable of capturing a greater variety of behaviours and dynamics, such as power-law decay, sub- diffusion, and super-diffusion, since they permit derivatives of non-integer orders.

- **Anomalous Diffusion and Transport :-**

  When memory effects, spatial heterogeneity, and complicated boundary conditions are present, anomalous diffusion processes like sub diffusion and super diffusion emerge. Fractional differential equations provide a suitable framework for explaining these processes.

- **Control and Optimization :-**

  With the use of FDEs, fractional-order controllers with better transient response, stronger disturbance rejection, and larger stability margins can be designed with desirable characteristics.

- **Signal Processing and Image Analysis :-**

  In signal processing and image analysis, fractional calculus is essential because it offers useful tools for modelling and examining non-stationary signals, fractal patterns, and multi-scale phenomena.

- **Stochastic Processes and Random Media :-**

  Applications of fractional differential equations include the modelling of stochastic processes and random media, where they offer a framework for explaining the behaviour of intricate systems that are inherently uncertain and random.

2.2 Applications of Fractional Differential Equations

Fractional differential equations (FDEs) have found use in a broad variety of scientific, engineering, and mathematical topics because of their capacity to represent non-local and memory-dependent behaviours. Detailed FDE applications in a range of fields are as follows,

1. **Physics and Mechanics :-**

   - **Viscoelasticity :-** The behaviour of viscoelastic materials, such as gels, polymers, and biological tissues, is modelled using FDEs. The relaxation phenomena and memory effects seen in these materials are explained by the fractional derivatives.
   - **Diffusion Processes :-** Particle movement in complicated mediums where the classical diffusion equation fails is described by FDEs in anomalous diffusion.
   - **Fractal Geometry :-** Fractal objects, which have non-integer dimensions, are modelled using FDEs. Natural phenomena such as snowflakes, turbulence, and coastlines are examples of fractals.

2. **Engineering :-**

   - **Control Systems :-** Fractional-order models are utilised in estimation and prediction algorithms, where fractional calculus is used to estimate system parameters and forecast future system behaviour.
   - **Electrochemical Systems :-** Supercapacitors, fuel cells, and batteries' charge and ion transfer are all explained by FDEs. Accurately modelling these systems aids in the creation of energy storage devices with higher efficiency.

- **Signal Processing :-** In signal processing, fractional calculus is used for filtering, denoising, and simulating signals with long-term memory. It can be used for seismic data analysis, speech recognition, and picture processing.

3. **Biology and Medicine :-**

   - **Biological Kinetics :-** FDEs are used to simulate how medications and medicines are distributed, metabolised, and eliminated from the human body. Enzyme catalysis and interactions with substrates are described using FDEs.
   - **Neuroscience :-** FDEs are employed in the study of brain signals, including data from functional magnetic resonance imaging (fMRI) and electroencephalography (EEG). In order to simulate non-Gaussian and non-stationary behaviour in brain signal time series, fractional derivatives are useful.
   - **Bioinformatics :-** Molecular biology uses FDEs to describe the evolution of genes and proteins, taking memory effects and non-local interactions into consideration.

4. **Cybersecurity :-**

   - **Anomaly Detection :-** FDEs are useful for simulating system operations, user behaviour, and network traffic patterns. Fractional-order modelling can be used to find possible security breaches, abnormalities, and departures from typical behaviour.
   - **Intrusion Detection :-** FDEs help intrusion detection systems (IDS) by simulating predicted network or system behaviour
   - **Advanced Persistent Threat (APT) Detection :-** Long-term cyberattacks known as advanced persistent threats (APTs) aim to stay hidden for extended periods of time.

5. **Environmental Science :-**

   - **Hydrology :-** FDEs improve predictions for water resource management and environmental protection by modelling groundwater flow and pollution transport in aquifers with memory effects.

- **Environmental Modelling :-** FDEs are used to model complicated environmental systems, such as the spread of pollutants in rivers and lakes and air quality modelling.

6. **Electromagnetics :-**

   - **Electromagnetic Wave Propagation :-** Wave propagation in complex media, such dispersive materials and fractal antennas, is described by FDEs.

7. **Chemical Engineering :-**

   - **Chemical Reactor Modelling :-** The behaviour of reactors exhibiting non-local and memory-dependent properties is described using FDEs.

8. **Geophysics :-**

   - **Seismology :-** Taking into account the non-local nature of seismic waves, FDEs aid in modelling the propagation of seismic waves in the Earth's crust.

9. **Robotics :-**

   - **Robot Control :-** Robotic systems use fractional-order controllers based on FDEs for more precise and flexible control, particularly for tasks demanding dexterity and compliance.

2.2.1 Literature Review of FDE

Agarwal et al. [17] have surveyed impulsive and stable Caputo Fractional Differential Equations with discussing the types of Fractional Differential Equations. Podlubny [18] have discussed on Some basic Theorems and Numerical Methods of Fractional Differential Equations. Skovranek et al. [19] Compared the Fractional Order model and Integer order model for Data fitting using the solutions of Fractional Differential Equation. Ford and Simpson [20] have studied the numerical solutions of Fractional differential Equations for speed versus accuracy. Rahimy [21] have studied the Applications of Fractional Differential Equations.

2.3 Some Basic Theorms

1. Consider the system,

$$ {}_{t_0}^{c}D_t^{\alpha}x(t) = g(t,x), t > t_0 $$

Let us consider the initial condition as $x(t_0), where\ 0 < \alpha \leq 1$ and $g : [t_0, \infty] \times \Omega \to R^n, \Omega \in R^n$. When g(t,x) holds the locally Lipchitz conditions concerning x, then the above equation has a unique solution on $[t_0, \infty) \times \Omega$

2. Let $0 < \alpha \leq 1$. Suppose that $g(t) \in C(a,b)$ and

$$ {}^{c}D_t^{\alpha} g(t) \in C(a,b) $$

If ${}^{c}D_t^{\alpha} g(t) \geq 0, \forall t \in (a,b)$ then $g(t)$ is non-decreasing function for each $t \in (a,b)$.
If ${}^{c}D_t^{\alpha} g(t) \leq 0, \forall t \in (a,b)$ then $g(t)$ is non-increasing function for each $t \in (a,b)$.

3. Let g(t) be a continuous function on $[t_0, \infty]$ which satisfies

$$ {}_{t_0}^{c}D_t^{\alpha} g(t) \leq -\lambda g(t) + \xi \quad , \quad g(t_0) = g_{t_0} $$

Here, $0 < \alpha \leq 1, (\lambda, \xi)\, \epsilon R^2$ and $\lambda \neq 0$. Let us consider $t_0 \geq 0$ as the initial time. Now,

$$ g(t) \leq \left(g(t_0) - \frac{\xi}{\lambda} \right) E_{\alpha}\left[-\lambda (t - t_0)^{\alpha} \right] + \frac{\xi}{\lambda} $$

4. Let $g(t) \in R^{+}$ be a derivable and continuous function. Then, at any time $t > t_0$,

$$ {}_{t_0}^{c}D_t^{\alpha} \left(g(t) - g^* - g^* \ln \frac{g(t)}{g^*} \right) \leq \left(1 - \frac{g^*}{g} \right) \quad {}_{t_0}^{c}D_t^{\alpha} g(t)\,,\ z\ g^* \in R_+,\ \forall a \in (0,1) $$

5. If g is a continuous function on [a,b], then the following conditions holds good on [a,b]

$$ \| \ {}_{t_0}^{ABC}D_t^{\alpha} g(t) \| < \frac{B(\alpha)}{1-\alpha} \ \| g(t) \|, where \| g(t) \| = \ max_{0 \leq t \leq 1} \| g(t) \| $$

6. The ordinary differential equation with time-fractional ${}_{t_0}^{ABC}D_t^{\alpha} g_1(t) = u(t)$ has a unique solution denoted as,

$$g(t) = g(t_0) + \frac{1-\alpha}{B(\alpha)} u(t) + \frac{\alpha}{B(\alpha)\Gamma(\alpha)} \int_a^t u(\tau)(t-\tau)^{\alpha-1} d\tau$$

7. Atangana-Baleanu Caputo represented in equation (1) derivative satisfy the Lipschitz condition,

$$\| \ {}_a^{ABC}D_t^{\alpha} g_1(t) - {}_a^{ABC} D_t^{\alpha} g_2(t) \| < \phi_1 \| g_1(t) - g_2(t) \|$$

2.4 Numerical Methods

Adams-Bashforth-Moulton Method using Caputo Sense :-

Consider the non-linear fractional differential equation with the initial conditions,

$$^{C}D_t^{\alpha} x(t) = \phi(t, x(t)), 0 \leq t \leq T$$

$$x^{(m)}(0) = x_0^{(m)}, m = 0, 1, 2, 3, ..., \nu .., \nu = \lceil \alpha \rceil.$$

The corresponding Volterra integral equation may be written as

$$x(t) = \sum_{m=0}^{v-1} x_0^{(m)} \frac{t^m}{m!} + \frac{1}{\Gamma(\alpha)} \int_0^t (t-s)^{\alpha-1} \ \phi(s, x(s)) ds.$$

Set h=$\frac{T}{\mathbb{N}}$, $t_n = nh$, $n = 0, 1, 2, ..., \mathbb{N} \in Z^+$.

$$x_h(t_{n+1}) = \textstyle\sum_{i=0}^{n} x_0^{(\mathfrak{m})} \frac{t_{n+1}^m}{m!} \ + \frac{h^{\alpha}}{\Gamma(\alpha+2)} (\phi\left(t_{n+1}, x_h^P(t_{n+1})\right)$$

$$+ \sum_{i=0}^{n} a_{i,n+1} \phi(t_i, x_h(t_i))),$$

where,

$$x_h^P(t_{n+1}) = \sum_{m=0}^{v-1} x_0^{(m)} \frac{t_{n+1}^m}{m!} + \frac{1}{\Gamma(\alpha)} \sum_{i=0}^{n} b_{i,n+1} \phi(t_i, x_h(t_i)),$$

In which,

$$a_{i,n+1} = \begin{cases} n^{\alpha+1} - (n-\alpha)(n+1)^{\alpha} & \text{if } i = 0 \\ (n-i+2)^{\alpha+1} + (n-i)^{\alpha+1} - 2(n-i+1)^{\alpha+1} & \text{if } 1 \le i \le n \\ 1 & \text{if } i = n+1 \end{cases}$$

And

$$b_{i,n+1} = \frac{h^{\alpha}}{\alpha}\left((n-i+1)^{\alpha} - (n-i)^{\alpha}\right),\ 0 \le i \le n,$$

Adams-Bashforth-Moulton method in the Atangana-Baleanu sense:-

Consider the non-linear fractional differential equation with the initial conditions,

$$\begin{aligned} {}^{ABC}_{t_0}D^{\alpha}_{t}x(t) &= \phi(t, x(t)), 0 \le t \le T \\ x^{(m)}(0) &= x_0^{(m)}, \quad m = 0, 1, 2, 3, ..., \nu.., \nu = \lceil \alpha \rceil. \end{aligned}$$

The corresponding Volterra integral equation can be written as,

$$x(t) = \sum_{m=0}^{v-1} x_0^{(m)} \frac{t^m}{m!} + \frac{1}{\Gamma(\alpha)} \int_0^t (t-s)^{\alpha-1} \phi(s, x(s))\, ds.$$

Set $h = \frac{T}{\mathbb{N}},\ t_n = nh,\ n = 0, 1, 2, ..., \mathbb{N}\ \in Z.$

$$x_h(t_{n+1}) = \sum_{\mathrm{m=0}}^{\nu-1} x_0^{(m)} \frac{t_{n+1}^m}{\mathrm{m!}} + \frac{1-\alpha}{\mathrm{B}(\alpha)}(\phi(t_{n+1}, x_h(t_{n+1})))$$

$$+\frac{\alpha \mathrm{h}^{\alpha}}{\mathrm{B}(\alpha)\Gamma(\alpha\ +\ 2)}(\phi(t_{n+1}, \mathrm{x_h^P}(t_{n+1})) + \sum_{\mathrm{i=0}}^{n} \mathrm{a_{i,n+1}}\phi(t_i, x_h(t_i))).$$

Where,

$$x_h^P(t_{n+1}) = \sum_{\mathrm{m=0}}^{\nu-1} x_0^{(m)} \frac{t_{n+1}^m}{\mathrm{m!}} + \frac{1-\alpha}{\mathrm{B}(\alpha)}(\phi(t_{n+1}, x_h(t_{n+1})) + \frac{\mathrm{h}^{\alpha}}{\mathrm{B}(\alpha)\Gamma(\alpha)} \sum_{\mathrm{i=0}}^{\mathrm{n}} \mathrm{b_{i,n+1}}\phi(t_i, x_h(t_i)),$$

In which,

$$a_{i,n+1} = \begin{cases} n^{\alpha+1} - (n-\alpha)(n+1)^{\alpha} & \text{if } i = 0 \\ (n-i+2)^{\alpha+1} + (n-i)^{\alpha+1} - 2(n-i+1)^{\alpha+1} & \text{if } 1 \leq i \leq n \\ 1 & \text{if } i = n+1 \end{cases}$$

And

$$b_{i,n+1} = \frac{h^{\alpha}}{\alpha}\left((n-i+1)^{\alpha} - (n-i)^{\alpha}\right),\ 0 \leq i \leq n,$$

3 Fractional Analysis of Transmission Model on the spread of Covid-19 - A Case Study

3.1 Introduction

The uncontrolled rise in the incidence of SARS-CoV-2 has prompted the adoption of mitigation measures of an unprecedented magnitude worldwide since March 2020. A number of reports using "epidemic modeling" highlighted the dire perspective of an acute infectious disease saturating the health system, an unexpected situation in developed countries where the healthcare system focuses on chronic diseases. One particularly encouraging report was released by Imperial College scientists at the end of February 2020, announcing the overwhelming capacity for acute care and the need for long-term, severe social distancing measures to combat the disease. This announcement aided governments worldwide in combating the disease.

We are analysing this Model by the article Bhaishya et al. [22]

3.2 Model Formulation

This study uses the popular susceptible-exposed-infectious-recovered (SEIR) model to show how the deadly Coronavirus evolved. Taking note of the current state of human infection,

We have added vaccination segment also as it is being introduced in many nations in an effort to create a more realistic model. The entire size of the human population on Earth is represented in the model formulation by $N_c(t)$, which is further divided into five classes at any given moment t: exposed $E_c(t)$, susceptible $S_c(t)$, unreported $U_(t)$, infected $I_(t)$, and recovered $R_c(t)$.

$$N(t) = S_c(t) + E_c(t) + I_c(t) + U_c(t) + R_c(t).$$

The vaccinated population are considered to be a non-vulnerable group in this model and are denoted by V(t). The interaction diagram of the population is projected in Figure [**??**]. The arrows indicate the amount of population moving from one segment to another.

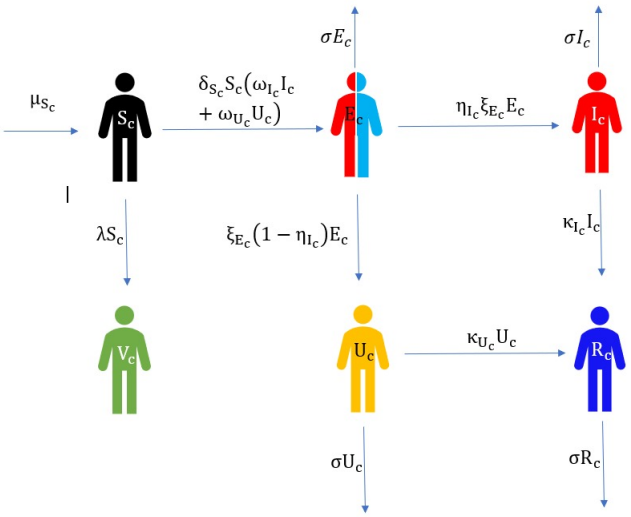

Figure 9: Figure of interaction among various groups of population

All assumptions of the COVID-19 model discussed [2] can be stated below:

1. Susceptible comes to contact by an infected or unreported group, who are expected to be exposed to the disease and at the rate of $vS_c(\phi_1 +$

$\phi_2)(I_c + U_c)$ move to the exposed population.

2. Exposed population turns to the infected segment and the unreported population at the rate of $\eta_{I_c}\xi_{E_c}E_c$ and $\xi_{E_c}(I_c - \eta_{I_c})E_c$ respectively.

3. The infected and unreported populations turns into the recovery segment at the rate of $\kappa_{I_c}I_c$ and $\kappa_{U_c}U_cS_c$ respectively.

4. Susceptible population gets vaccinated at the rate of λS_c.

with $S_c(t) > 0, E_c(t) > 0, I(t) > 0, U_c(t) > 0, R_c(t) > 0$ and $V_c(t) > 0$ and where t_0 is the initial time. All the parameters $\mu_S, \delta_S, \omega_I, \omega_U, \lambda, \xi_E, \sigma, \eta_I, \kappa_I, \kappa_U$ are positive whose biological meanings are mentioned in table 3.2:

μ_{S_c}	n × N, n is the birth rate and N is the total population of world
δ_{S_c}	Contact rate
ω_{I_c}	Disease transmission rate from I_c
ω_{U_c}	Disease transmission rate from U_c
λ	Vaccination rate
ξ_{E_c}	Rate of exposed population being infected
σ	Natural death rate of humans
η_{I_c}	Rate at which E_c progresses to I_c
κ_{I_c}	Recovery rate of infected population
κ_{U_c}	Recovery rate of unreported population

Table 1: Meaning of the symbols used in the model (2)

$$
\begin{aligned}
{}^{ABC}_{t_0}D^{\alpha}_{t} S_c &= \mu_{S_c} - \delta_{S_c}S_c(\omega_{I_c}I_c + \omega_{U_c}U_c) - \lambda S_c, \\
{}^{ABC}_{t_0}D^{\alpha}_{t} E_c &= \delta_{S_c}S_c(\omega_{I_c}I_c + \omega_{U_c}U_c) - \xi_{E_c}E_c - \sigma E_c, \\
{}^{ABC}_{t_0}D^{\alpha}_{t} I_c &= \eta_{I_c}\xi_{E_c}E_c - \kappa_{I_c}I_c - \sigma I_c, \\
{}^{ABC}_{t_0}D^{\alpha}_{t} U_c &= \xi_{E_c}(1 - \eta_{I_c})E_c - \kappa_{U_c}U_c - \sigma U_c, \\
{}^{ABC}_{t_0}D^{\alpha}_{t} R_c &= \kappa_{I_c}I_c + \kappa_{U_c}U_c - \sigma R_c, \\
{}^{ABC}_{t_0}D^{\alpha}_{t} V_c &= \lambda S_c
\end{aligned}
\tag{2}
$$

- The solution of the system of fractional differential equations [2] exists and is unique.

BR Number :-

Basic Reproduction Number(BR Number) denoted by R_0, BR Number of an infection is the expected number of cases directly generated by one case in a population where all individuals are susceptible to infection.On solving the system [2], we obtain the disease-free equilibrium (DFE) point $E_0 = (\frac{\mu_s}{\lambda}, 0, 0, 0, 0)$. DFE point is $E_0 = (\frac{\mu_s}{\lambda}, 0, 0, 0, 0)$. We compute the BR number by evaluating the next generation matrix. To compute BR number R_0, we obtain the disease-free equilibrium (DFE) point $E_0 = (\frac{\mu_s}{\lambda}, 0, 0, 0, 0)$. DFE point is $E_0 = (\frac{\mu_s}{\lambda}, 0, 0, 0, 0)$. We get the BR number by evaluating the next generation matrix.

$$R_0 = \frac{\xi_{E_c}\delta_{S_c}\mu_S\left(\eta_{I_c}\omega_{I_c}\left(\sigma+\kappa_{U_c}\right)+(1-\eta_{I_c})\omega_{U_c}\left(\sigma+\kappa_{I_c}\right)\right)}{\lambda\left(\xi_{E_c}+\sigma\right)\left(\sigma+\kappa_{I_c}\right)\left(\sigma+\kappa_{U_c}\right)}$$

Sensitivity Analysis of R_0:-

Sensitivity analysis of the BR number indicates that by controlling the contact rate and transmission rate, and by improving the recovery rate and vaccination rate the disease can be controlled from being endemic. we have analyzed the sensitivity of the BR number by evaluating the first derivative of BR number with respect to various parameters

$$\frac{\partial R_0}{\partial \lambda} = -\frac{\xi_{E_c}\delta_{S_c}\mu_{S_c}\left(\eta_{I_c}\omega_{I_c}\left(\sigma+\kappa_{U_c}\right)+(1-\eta_{I_c})\omega_{U_c}\left(\sigma+\kappa_{I_c}\right)\right)}{\lambda^2\left(\xi_{E_c}+\sigma\right)\left(\sigma+\kappa_{I_c}\right)\left(\sigma+\kappa_{U_c}\right)}$$

3.3 Graphical Analysis

Numerical Simulations :- This section discusses the numerical simulation of the fractional COVID 19 Model [2] using real world data. The world's population as of April 21, 2021, was estimated by the WHO to be N = 7,84,52,61,000 = 7.9×10^9, with a birth rate of 17.873 births per 1,000 people. Thus, we have $\mu_{S_c} = \frac{n\times N}{365} = 384159.86\times365$ for each day. The list of COVID 19 instances worldwide as of April 21, 2021 is as follows:

Date	Rate of Vaccination
Before Jan 19	0.0003
Jan 19 to 31	0.001
Feb 10	0.003
Feb 20	0.005
Feb 28	0.007
Mar 10	0.009
Mar 20	0.013
Mar 30	0.016
April 21	0.028
April 30	0.035
May 10	0.042
May 20	0.049
May 30	0.055
June 10	0.063
June 20	0.072
June 30	0.082
July 10	0.093
July 20	0.104
July 30	0.117
Aug 10	0.13
Aug 20	0.243
Aug 30	0.272
Sept 10	0.300
Sept 20	0.322

Table 2: Vaccination Rate by months:

Targeted Population	Number of People
Total Confirmed Cases	14,31,23,631
Total Deaths	30,45,018
Total Recovery Cases	8,21,17,879
Fully Vaccinated	20,79,78,809
$S_{c_0}(t)$	0.7045×10^9
$E_{c_0}(t)$	0.2873×10^9
$I_{c_0}(t)$	0.1432×10^9
$U_{c_0}(t)$	0.2875×10^9
$R_{c_0}(t)$	0.082×10^9
$V_{c_0}(t)$	0.208×10^9
μ_{S_c}	384159.86
δ_{S_c}	2.7×10^{-8}
ω_{I_c}	0.01824
ω_{U_c}	0.012
λ	0.028
ξ_{E_c}	0.05965
σ	58.28×10^{-6}
η_{I_c}	0.955
κ_{I_c}	0.5737
κ_{U_c}	0.46

Table 3: WHO April 2021 Covid-19 Data Worldwide

To observe the impact of FD's on different populations, we have plotted the time history graphs of $S_c(t), E_c(t), I_c(t), U_c(t), R_c(t)$, and $V_c(t)$ for $\alpha = 1$, 0.9, 0.85, 0.8, and 0.7 using the aforementioned data and the fractional predictor-corrector technique. The population is estimated to be in the billions. Figure [10] illustrates how the addition of FDs makes all populations behave more realistic. Global data on infected, recovered, and unreported cases allows us to verify the model's validity even in the absence of readily available data on susceptible, exposed, and unreported cases. When derivative values are fractional-order instead of integer-order, Figures [10](c), [10](d), and [10](e) roughly represent the same number. A better representation is provided by $\alpha = 0.8$ and 0.7 than by other values of α. We have resorted to the WHO website as a point of comparison.

Since April and May of 2021 had the highest number of COVID-19 infections in India, the anticipated peak date in India might be regarded as the global peak. According to Figure [10](c)'s study of model [2]), the peak period of infection is May 1, 2021. However, examining the infection pattern as of May 10, 2021, which is represented at $\alpha = 0.7$, is more plausible. Figure [10] illustrates how the population of people who are immune to the virus and have received vaccinations rises while the population of people who are susceptible, exposed, infected, and unreported falls as the number of days grows. It is seen that, as the number of days grows, the infection reaches its peak and progressively declines because of the influence of vaccination. It is noted that the current model [2] illustrates how strongly the vaccination rate affects the containment of the COVID-19 pandemic.

GRAPHS :-

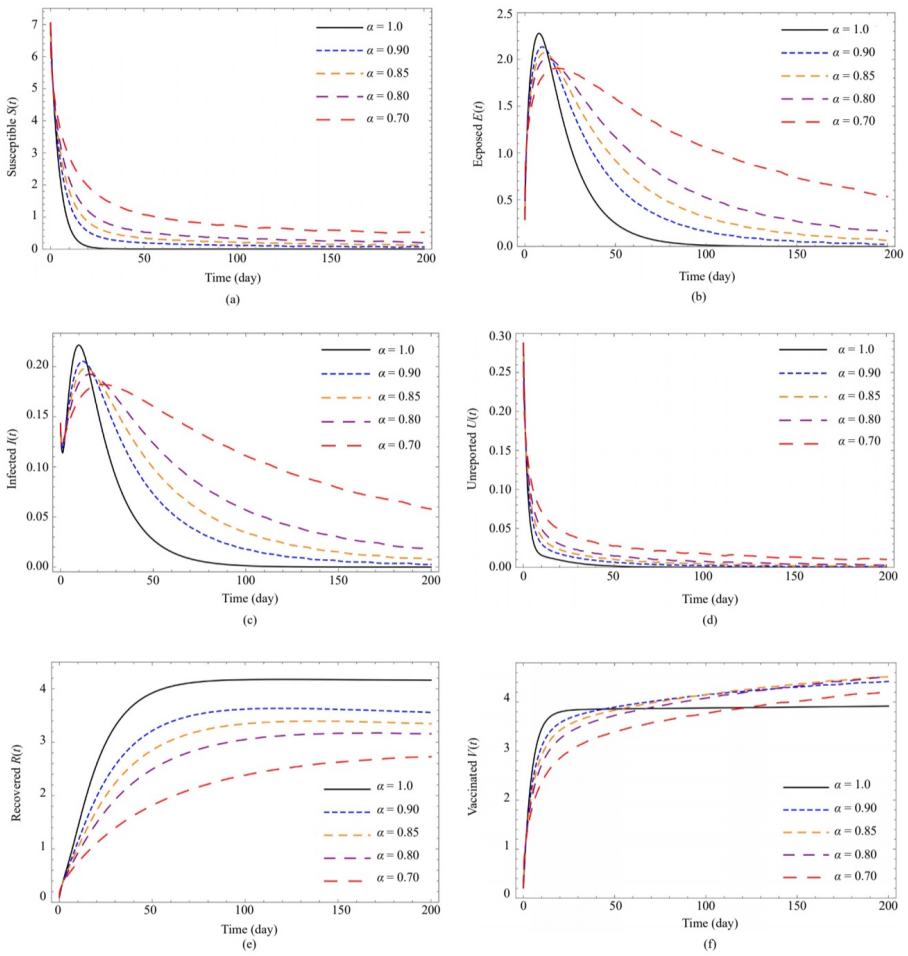

Figure 10: The Time History of (a) Susceptible S_c, (b) Exposed E_c, (c) Infected I_c, (d) Unreported U_c, (e) Recovered R_c and (f) Vaccinated V_c population for different values of α

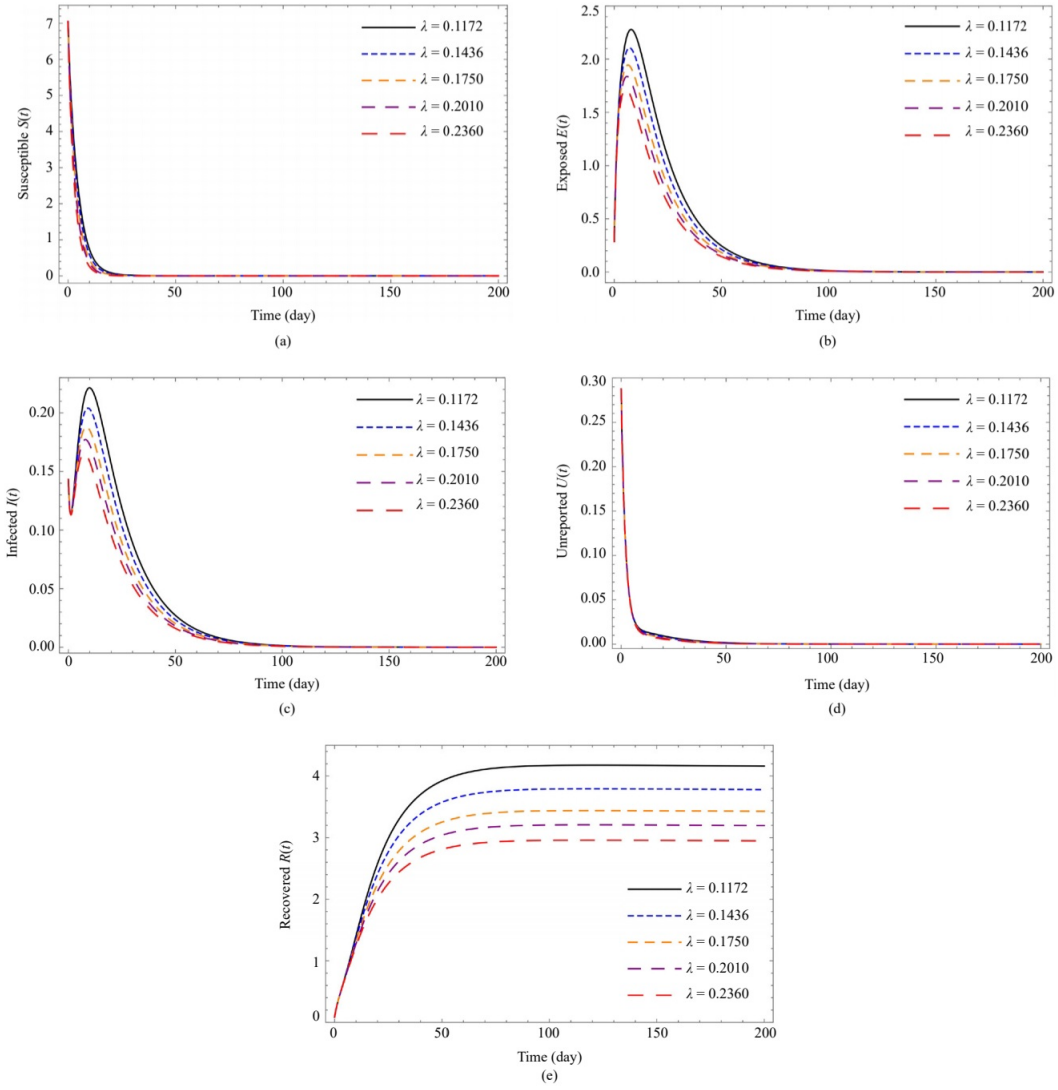

Figure 11: Effect after Vaccination on (a) Susceptible S_c, (b) Exposed E_c, (c) Infected I_c, (d) Unreported U_c and (e) Recovered R_c population for $\alpha = 1$

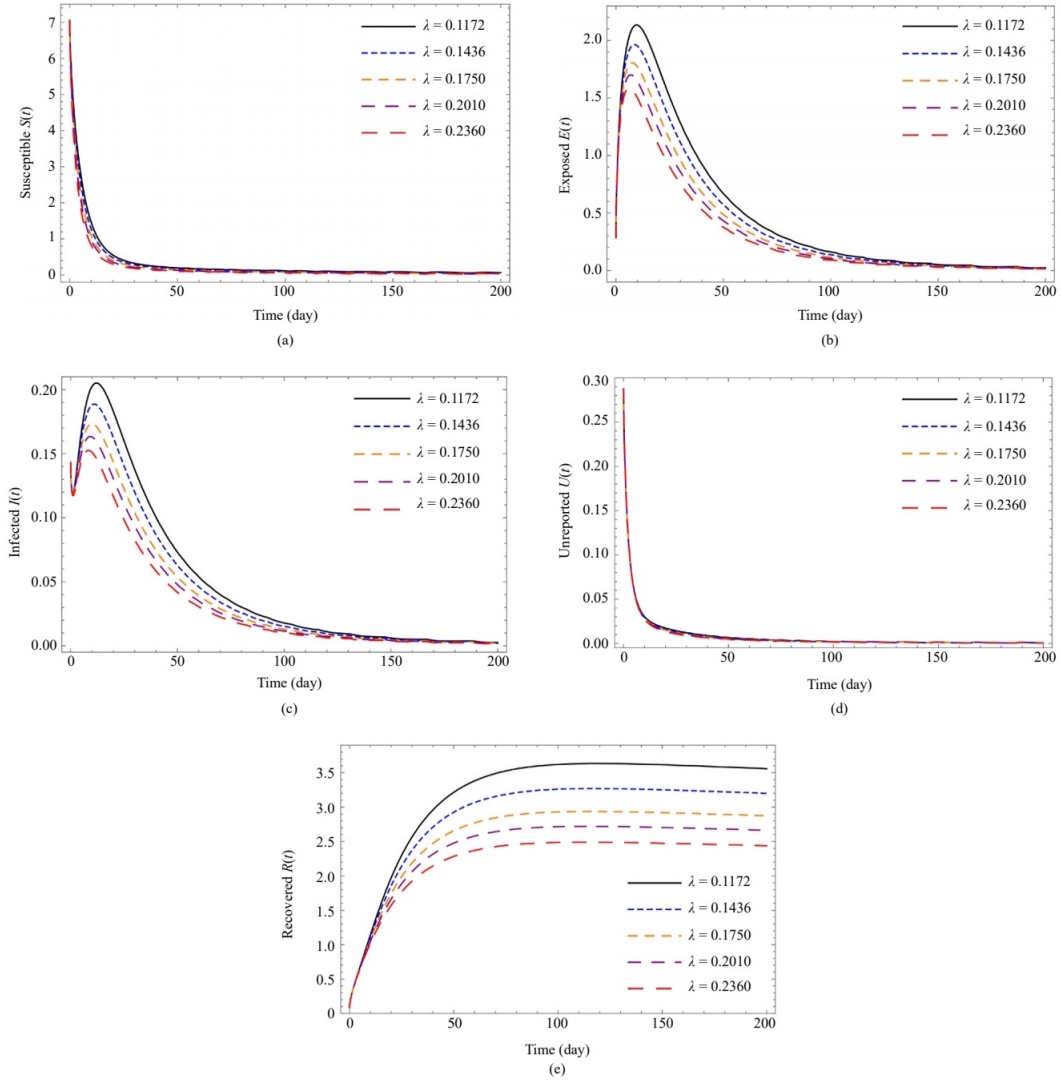

Figure 12: Effect after Vaccination on (a) Susceptible S_c, (b) Exposed E_c, (c) Infected I_c, (d) Unreported U_c and (e) Recovered R_c population for $\alpha = 0.9$

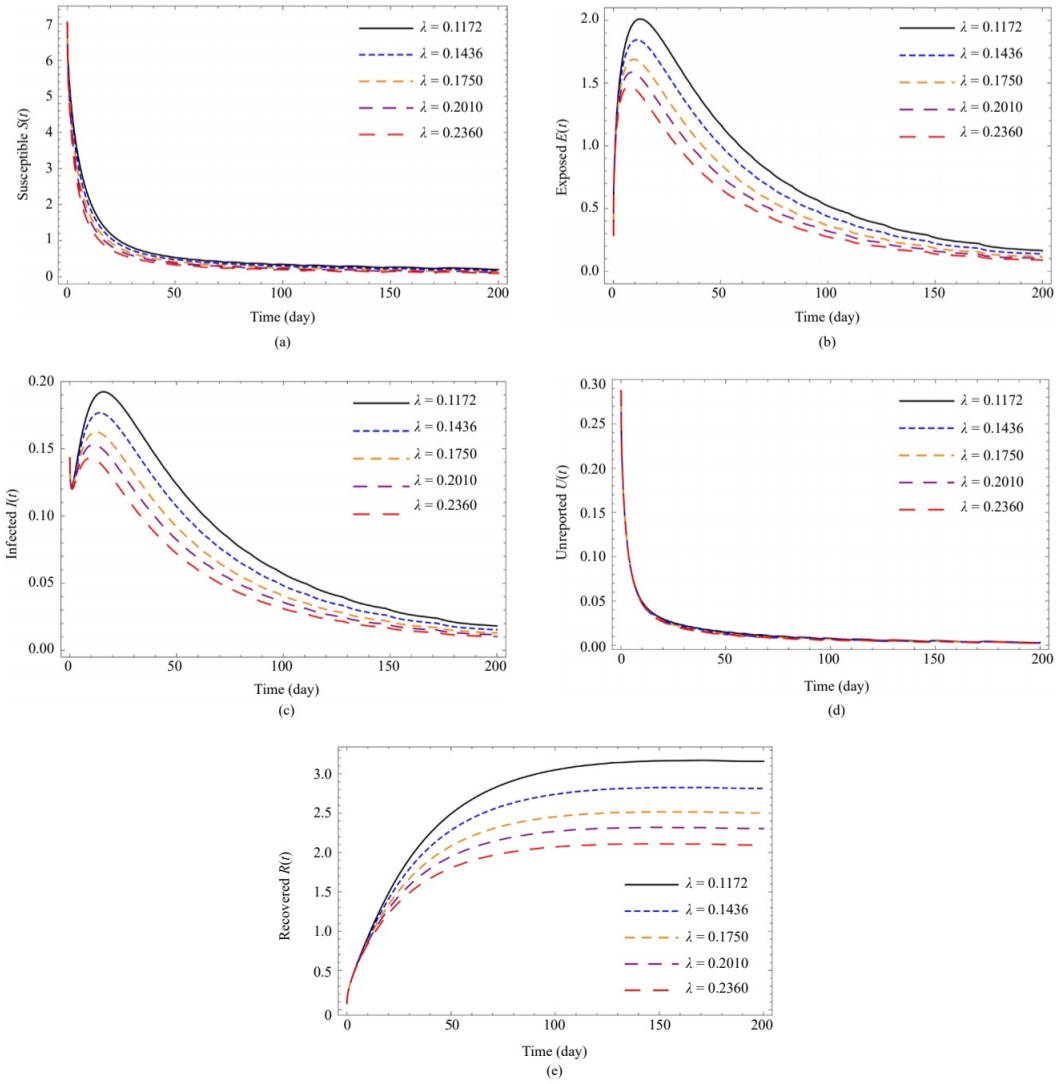

Figure 13: Effect after Vaccination on (a) Susceptible S_c, (b) Exposed E_c, (c) Infected I_c, (d) Unreported U_c and (e) Recovered R_c population for $\alpha = 0.8$

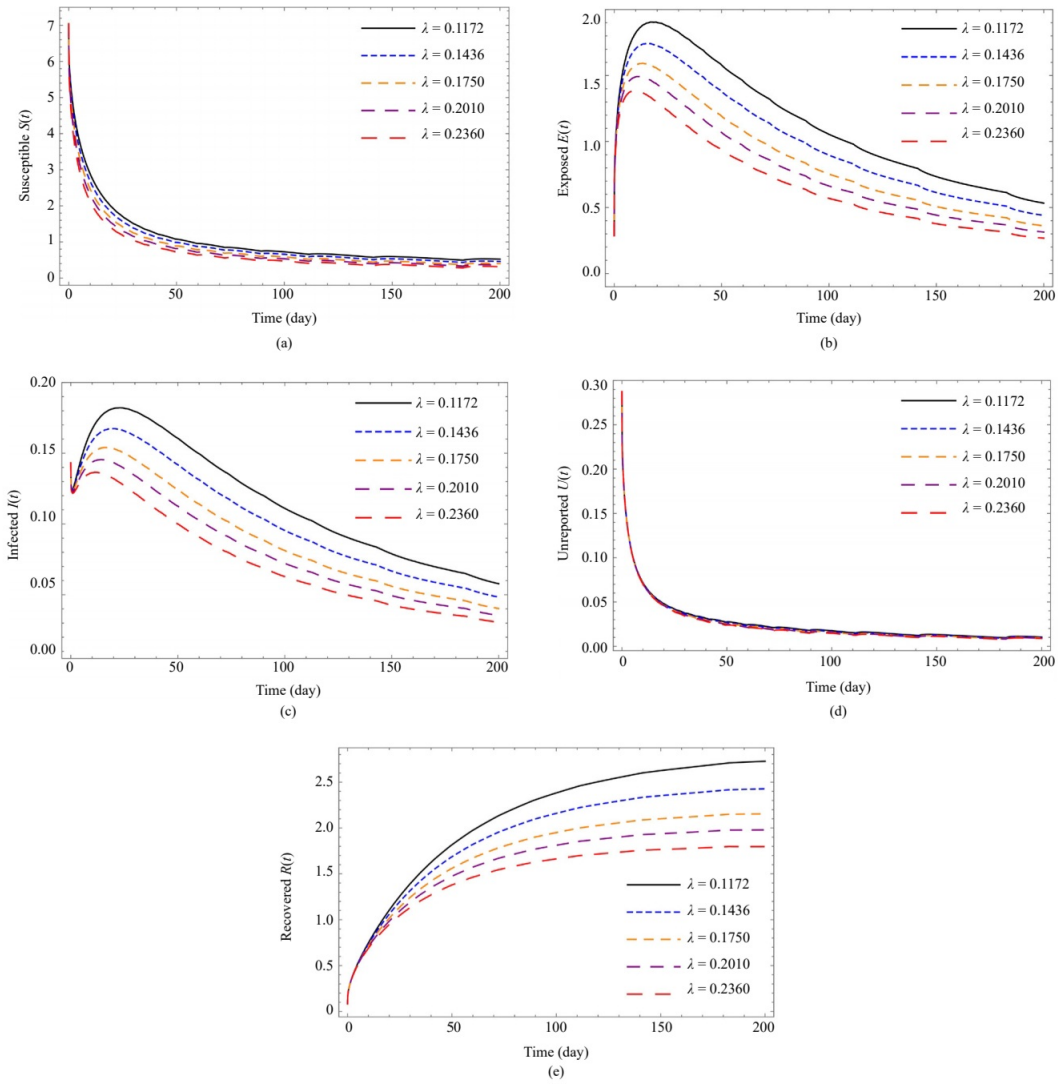

Figure 14: Effect after Vaccination on (a) Susceptible S_c, (b) Exposed E_c, (c) Infected I_c, (d) Unreported U_c and (e) Recovered R_c population for $\alpha = 0.7$

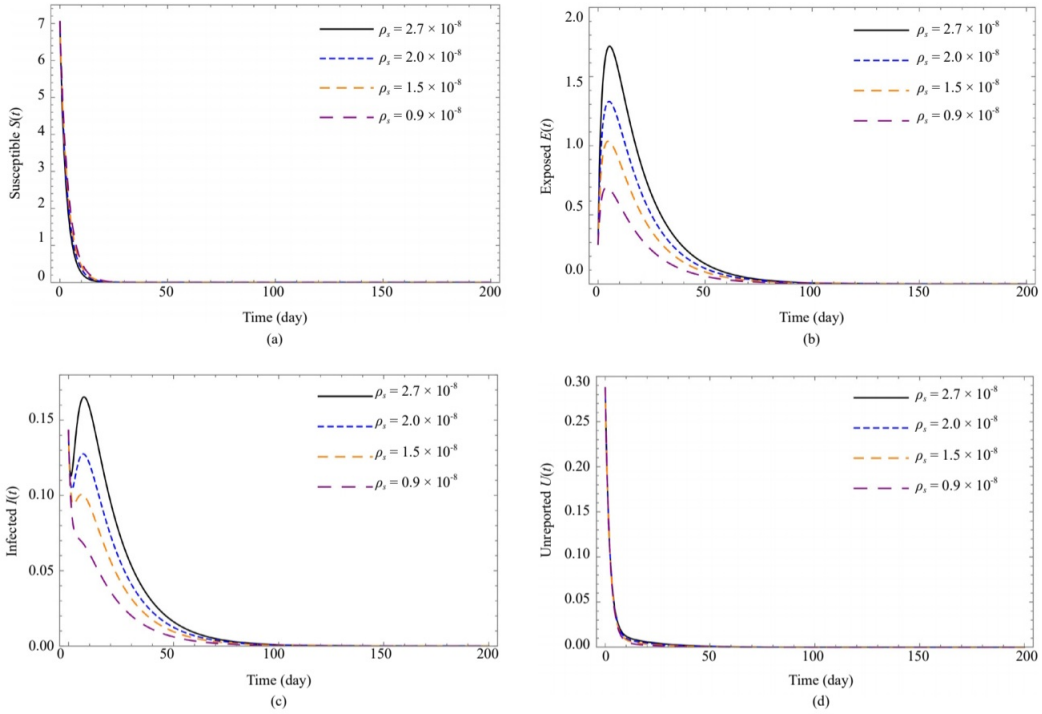

Figure 15: Effect of Contact Rate on (a) Susceptible S_c, (b) Exposed E_c, (c) Infected I_c and (d) Unreported U_c population for $\alpha = 1$

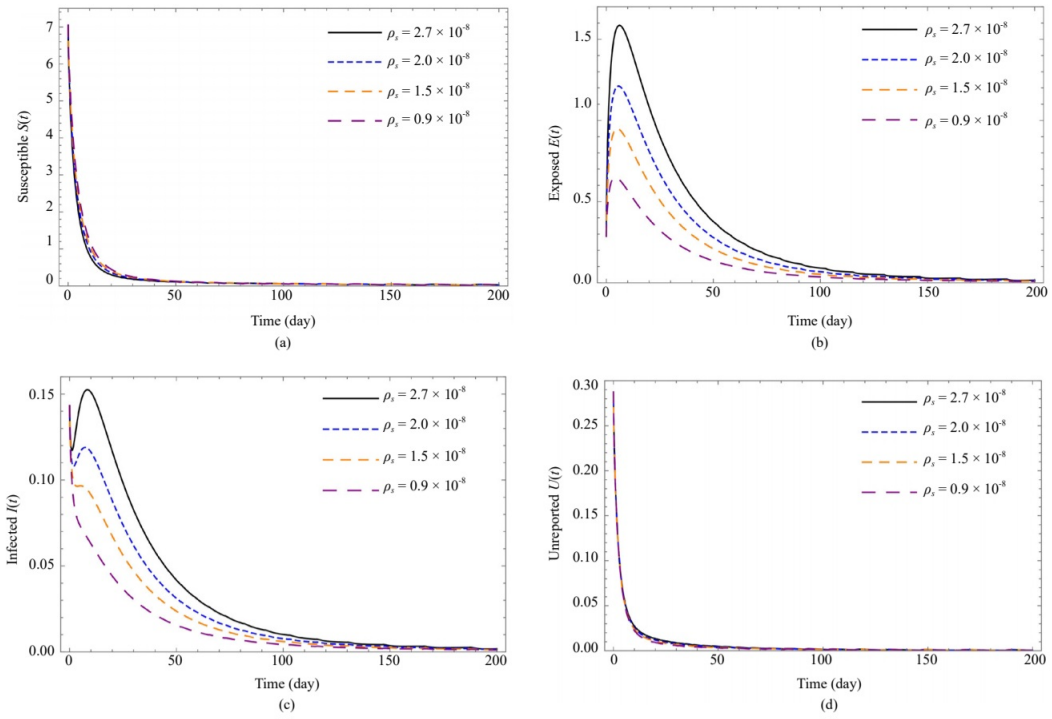

Figure 16: Effect of Contact Rate on (a) Susceptible S_c, (b) Exposed E_c, (c) Infected I_c and (d) Unreported U_c population for $\alpha = 0.9$

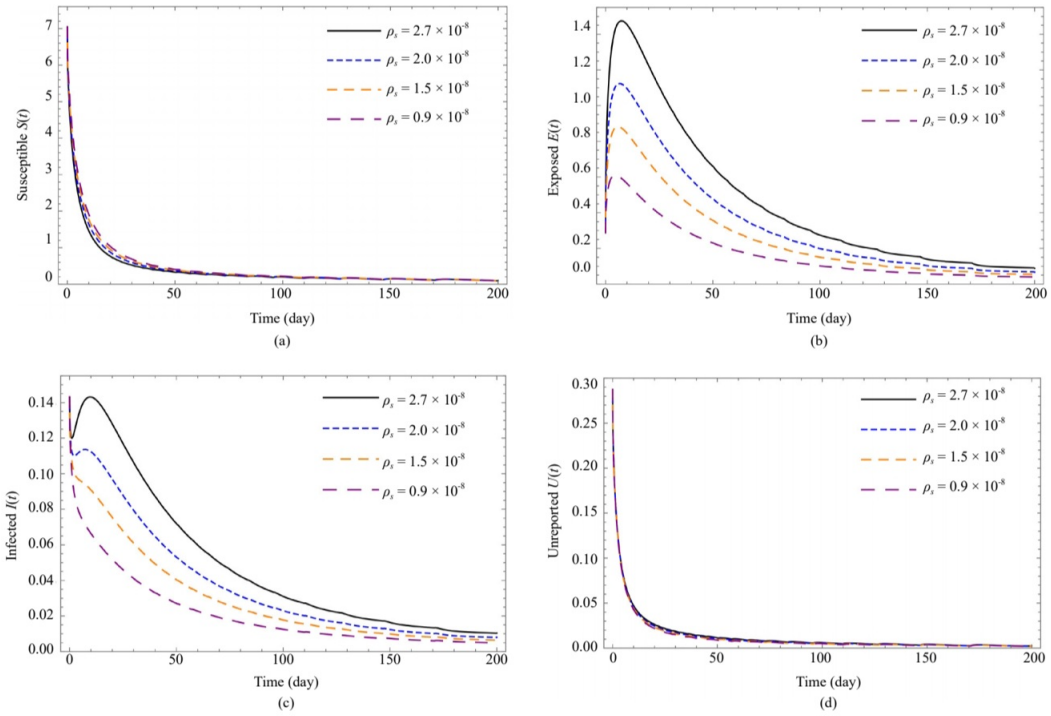

Figure 17: Effect of Contact Rate on (a) Susceptible S_c, (b) Exposed E_c, (c) Infected I_c and (d) Unreported U_c population for $\alpha = 0.8$

3.4 Conclusion

This study primarily analyzes a mathematical model for predicting the spread of COVID-19 disease. Included in the analysis is a vaccination drive in association with the Caputo fractional order derivative. We employed fixed point theory to examine the existence and uniqueness of potential solutions. The numerical investigation examines how COVID-19 evolves, how vaccination impacts it, and how contact rate affects its proliferation. We used WHO's data from 21 April 2021 as our starting point. Using the Caputo fractional operator in relation to susceptible, exposed, confirmed, unreported, recovered, and vaccinated populations influenced by the new virus provides insights into the implications of vaccination and contact rates on COVID-19. This understanding helps predict global changes related to the virus. In areas where vaccinations are widely provided there are observable patterns such as
(a) a decrease in severe illness from COVID19 as more people get vaccinated.
(b) small number and typically mild cases of "breakthrough infections" among fully vaccinated individuals.
(c) most serious cases resulting in hospitalization or death are found mainly among those who haven't been vaccinated.
A numerical test, using Mathematical and the predictor corrector method, yields solid results. Plots that use the fractional-order value for the derivative show a more persuasive pattern of disease progression than those using an integer-order derivative. This study highlights the value of mathematical models in addressing real-world issues and the efficiency of the fractional operator undergoing examination.

4 Mathematical Analysis of Pluviculture - A Fractional Approach - A Case Study

4.1 Introduction

One of the main problems that humanity is now experiencing is climate change. This is the long-term effect of global warming, which causes changes in rainfall and temperature. Rainmaking, also known as pluviculture, is the method of inducing precipitation artificially. This is done to stave off drought and to save Earth from global warming. This can be achieved using rockets or airplanes to sow to the clouds along with the catalysts like silver iodide, dry ice and salt powder, to increase precipitation and mitigate farmland drought. Aerosols stimulate the rain making process. Here we analyze the fractional mathematical model projecting pluviculture. The Caputo fractional derivative is used to improve the study of this occurrence. We examine the boundedness, existence, and uniqueness of the suggested system's solutions.

We are analysing this Model by the article Achar et al. [23]

4.2 Model Formulation

Here, we have used the Caputo fractional order derivative to analyse the fractional pluviculture model, which was inspired by the mathematical models of the artificial precipitation process. Six interacting variables control the pluviculture model: water vapour densities (C_V), rain drop densities (C_R), large size cloud droplets (C_{LD}), small size cloud droplet densities (C_{SD}), and concentrations of first and second type aerosols (C_1 and C_2, respectively).

$$
\begin{aligned}
&{}^{C}_{t_0}D^{\alpha}_{t} C_V = J_V - \rho_0 C_V - \rho_1 C_V C_1 \\
&{}^{C}_{t_0}D^{\alpha}_{t} C_{SD} = \phi_S C_V - \omega_{S_0} C_{SD} + \psi \rho_1 C_V C_1 - \phi_{S_1} C_{SD} C_2 \\
&{}^{C}_{t_0}D^{\alpha}_{t} C_{LD} = \phi_L C_{SD} - \phi_{L_0} C_{LD} + \phi_{S_1} C_{SD} C_2 - \phi_{L_1} C_{LD} C_2 \\
&{}^{C}_{t_0}D^{\alpha}_{t} C_R = \theta C_{LD} - \theta_0 C_R + \xi \phi_{L_1} C_{LD} C_2 \\
&{}^{C}_{t_0}D^{\alpha}_{t} C_1 = J_1 - \mu_1 C_1 - \rho_1 C_V C_1 \\
&{}^{C}_{t_0}D^{\alpha}_{t} C_2 = J_2 - \mu_2 C_2 - \phi_{S_1} C_{SD} C_2 - \phi_{L_1} C_{LD} C_2 - \phi_R C_R C_2
\end{aligned}
\tag{3}
$$

with initial condition $C_V(t_0) > 0,\ C_{SD}(t_0) > 0,\ C_{LD}(t_0) > 0,\ C_R(t_0) > 0,\ C_1(t_0) > 0,\ C_2(t_0) > 0$ where t_0 is the initial time. All the parameters $(J_V,\ \rho_0,\ \rho_1,\ \phi_S, \phi_{S_0},\ \psi,\ \phi_{S_1},\ \phi_L,\ \phi_{L_0},\ \phi_{L_1},\ \theta,\ \theta_0,\ \xi,\ J_1,\ J_2,\ \mu_1,\ \mu_2,\ \phi_R) > 0$

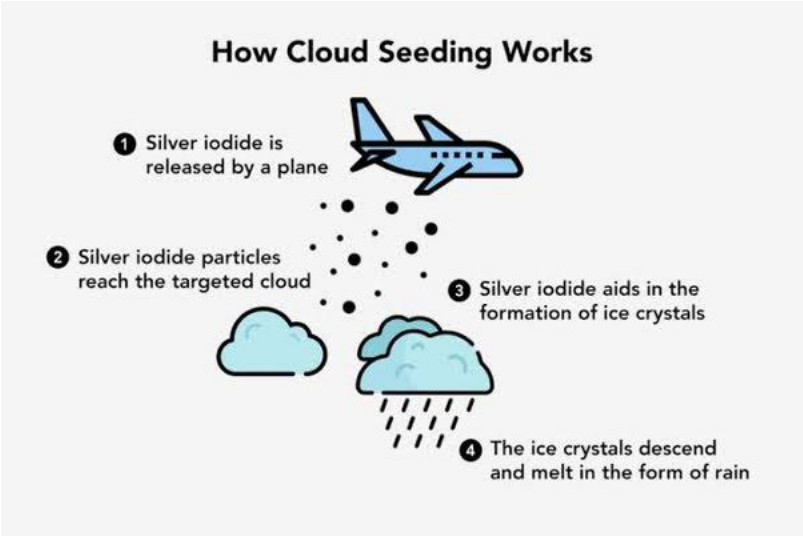

The water vapour phase is generated in the projected model [3] at a continuous basis at a rate of J_V (where the net rate of change in the water vapour density is assumed to be constant). At the rates J_1 and J_2, respectively, the first and second kinds of conductive aerosols are continually added to the environment. For $C_V, C_{SD}, C_{LD}, C_R, C_1 and\ C_2$, respectively, the constant terms $\rho_0,\ \phi_{S_0},\ \phi_{L_0},\ \theta_0,\ \mu_1\ and\ \mu_2$ signify the coefficients of natural reduction rate.

The rate of natural genesis of small size cloud droplets from water vapour, giant cloud drops from tiny cloud drops, and rain drops from large cloud drops is indicated by the equations $\phi_S \geq 0,\ \phi_L > 0,\ and\ r > 0$. Thus, it is evident that $r < \phi_{L_0}, \phi_L < \phi_{S_0}\ and\ \phi_S \leq \rho_0$. In terms of positive proportionality constants, the labels ψ and ξ are used. The rates of conversion between the water vapour phase and first kind aerosol, small and large cloud drop sizes and second kind aerosol, and raindrops and second kind aerosol are indicated by the coefficients $\rho_1,\ \phi_{S_1},\ \phi_{L_1}\ and\ \phi_R$, respectively.

- The Lipschitz condition holds good, therefore the solution of pluvivulture model [3] is unique
- The solution of the pluviculture model [3] exists by the fixed-point theorem
- The solutions of the pluviculture model [3] are uniformly bounded.
- Axial equilibrium point $\mathfrak{E}$ always exists and is always stable. Where,

$$\mathfrak{E} = (\frac{J_V}{\rho_0},\ 0,\ 0,\ 0,\ 0,\ 0)$$

- Aerosol free equilibrium point $\widetilde{\mathfrak{E}}$ always exists and is always stable. Where,

$$\widetilde{\mathfrak{E}} = (\widetilde{C}_V,\ \widetilde{C}_{SD},\ \widetilde{C}_{LD},\ \widetilde{C}_R,\ 0,\ 0)$$

4.3 Graphical Analysis

Numerical Simulations :-

Using the generalised Adams-Bashforth-Moulton technique, we have examined the dynamics of the projected fractional pluviculture model [3] by taking into account the parametric values $J_V \in (0,3),\ \rho_0 = 1,\ \rho_1 = 0.5,\ \phi_S = 0.1,\ \phi_{S_0} = 1,\ \psi = 1,\ \phi_{S_1} = 0.,\ \phi = 0.1,\ \phi_{L_0} = 1,\ \phi_{L_1} = 0.3,\ \theta = 0.1,\ \theta_0 = 0.02,\ \xi = 1$. With the initial conditions, $J_1 \in (0,3),\ J_2 \in (0,3),\ \mu_1 = 1,\ \mu_2 = 1\ and\ \phi_R = 0.01$. $C_R = 0.4919, C_V = 0.7545, C_{SD} = 0.2422, C_{LD} = 0.0862, C_1 = 0.6507, and C_2 = 0.8534$. Figures [18],[19] and [20] for $\alpha = 1$, 0.8, 0.5, respectively, show the variation in $C_V,\ C_{SD},\ C_{LD}\ and\ C_R$ for $J_V = 0,\ 1,\ 2,\ 3$. The natural generation of water vapour (J_V) is positively correlated with $C_V, C_{SD}, C_{LD}\ and\ C_R$. The growing trend is maintained as the fractional values are included, however the net value somewhat decreases.

Figures [21], [22] and [23] is for $\alpha = 1, 0.8, 0.5$ respectively, illustrates the variation in C_V , C_{SD}, C_{LD} and C_R for $J_1 = 0,\ 1,\ 2,\ 3$. Since less water vapour is naturally formed than is caused by first-kind particles, the value of C_V decreases as the rate of entry of these aerosols (J_1) into the environment increases. On the other hand, the increasing trend in the values of C_{SD}, C_{LD} and C_R indicates that this activity is stimulating the rainfall.

Figures [24],[25] and [26] for $\alpha = 1,\ 0.8,\ 0.5$ respectively, it illustrates the variation in $C_{SD},\ C_{LD}$ and C_R for $J_2 = 0,\ 1,\ 2,\ 3$. The value of C_{SD} decreases with an increase in the rate of entry of second type aerosols (J_2) into the environment because the creation of small drops is outweighed by the conversion of large drops to raindrops. As a result, the values of C_{LD} and C_R rise and cause the ecosystem to experience more rainfall than before.

The global stability of the $C_1-\ C_V$, $C_2-\ C_{SD}$, and C_2-C_{LD} spaces are for $\alpha = 1, 0.8$ respectively, is shown in Figures [27], [28] and [29]. Here, system [3]'s solution paths that begin in the domain of attraction reach equilibrium values.

GRAPHS :-

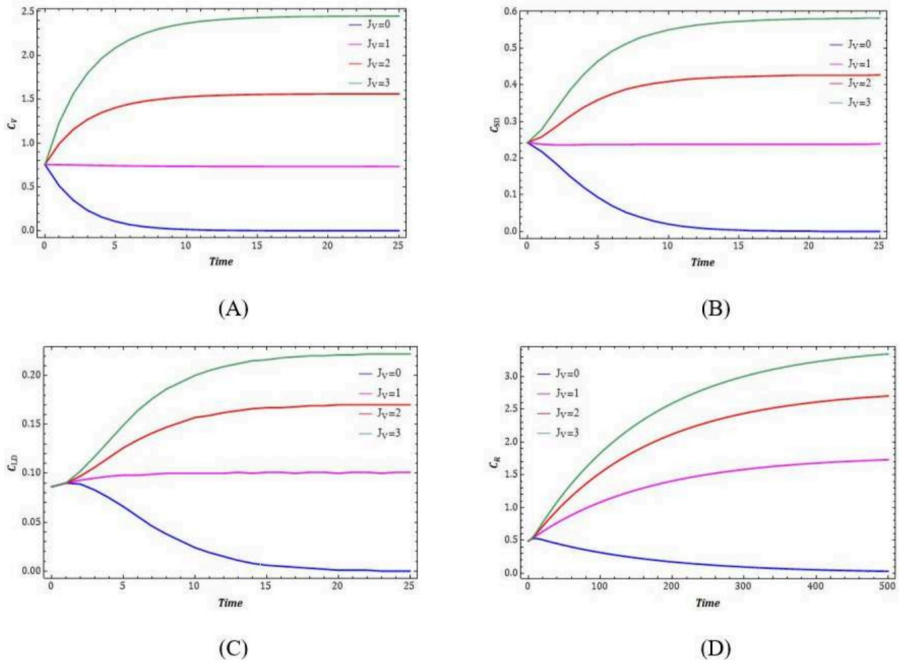

Figure 18: Variation in (A) C_V, (B) C_{SD}, (C) C_{LD} and (D) C_R for different values of J_V and $\alpha = 1$

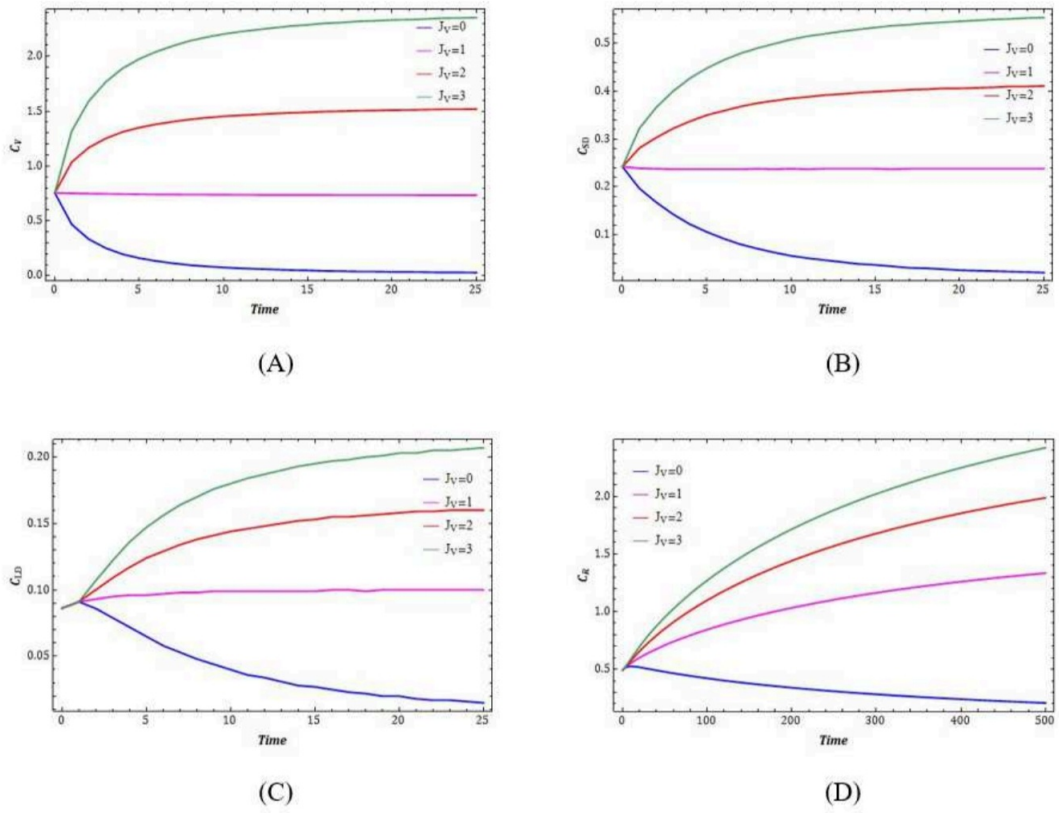

Figure 19: Variation in (A) C_V, (B) C_{SD}, (C) C_{LD} and (D) C_R for different values of J_V and $\alpha = 0.8$

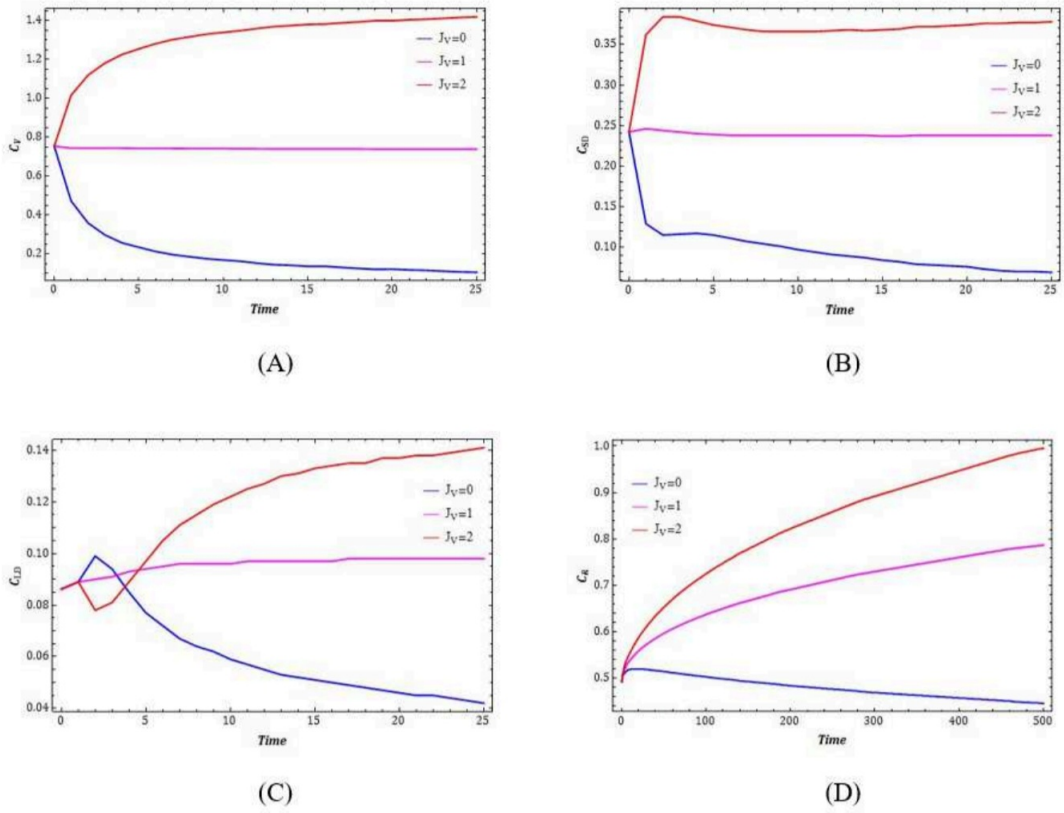

Figure 20: Variation in (A) C_V, (B) C_{SD}, (C) C_{LD} and (D) C_R for different values of J_V and $\alpha = 0.5$

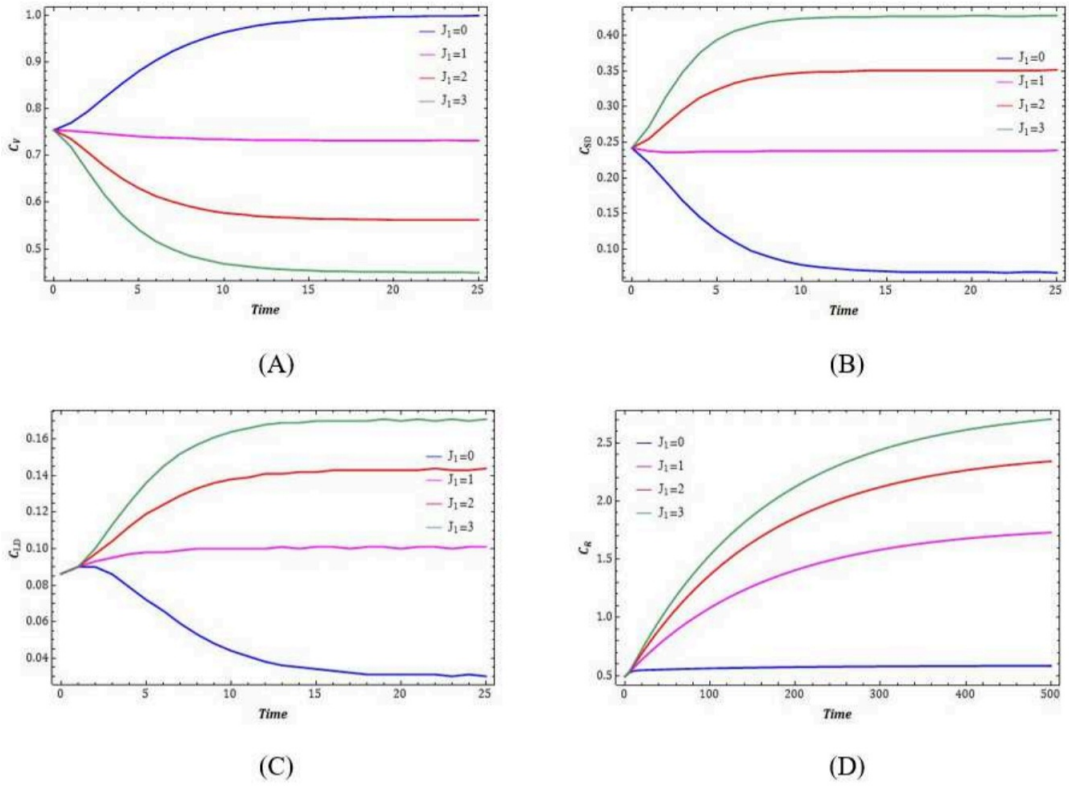

Figure 21: Variation in (A) C_V, (B) C_{SD}, (C) C_{LD} and (D) C_R for different values of J_1 and $\alpha = 1$

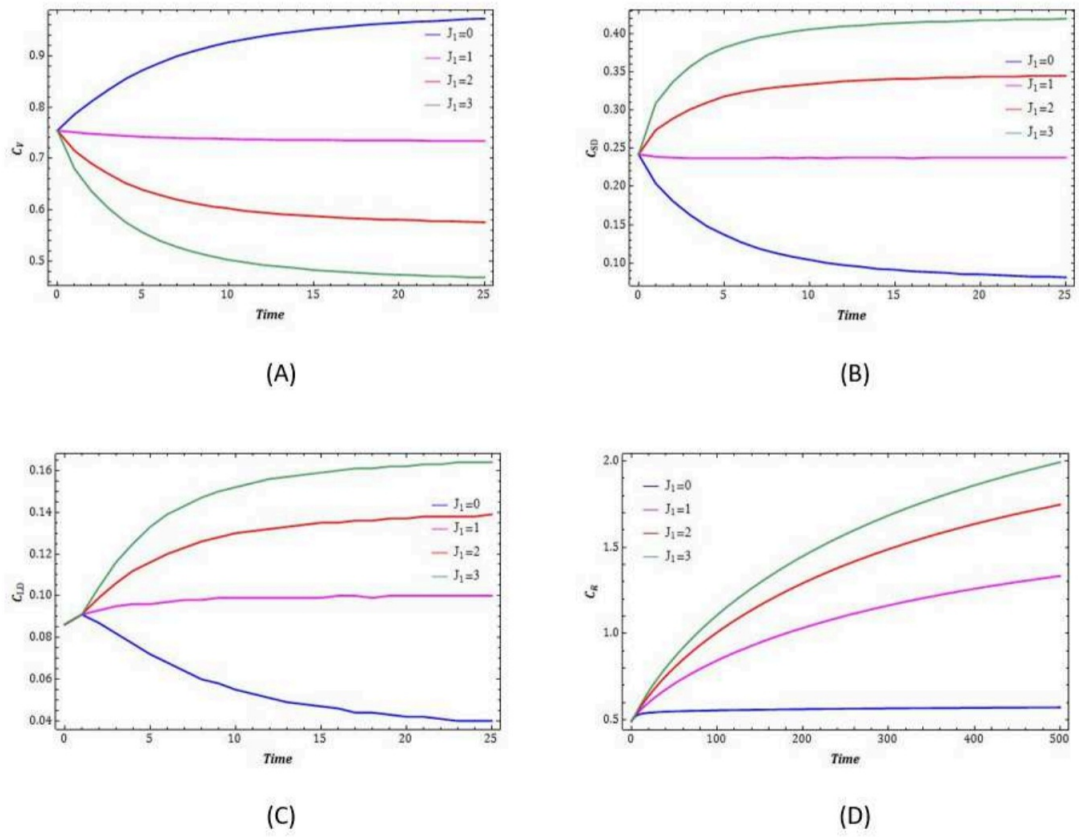

Figure 22: Variation in (A) C_V, (B) C_{SD}, (C) C_{LD} and (D) C_R for different values of J_1 and $\alpha = 0.8$

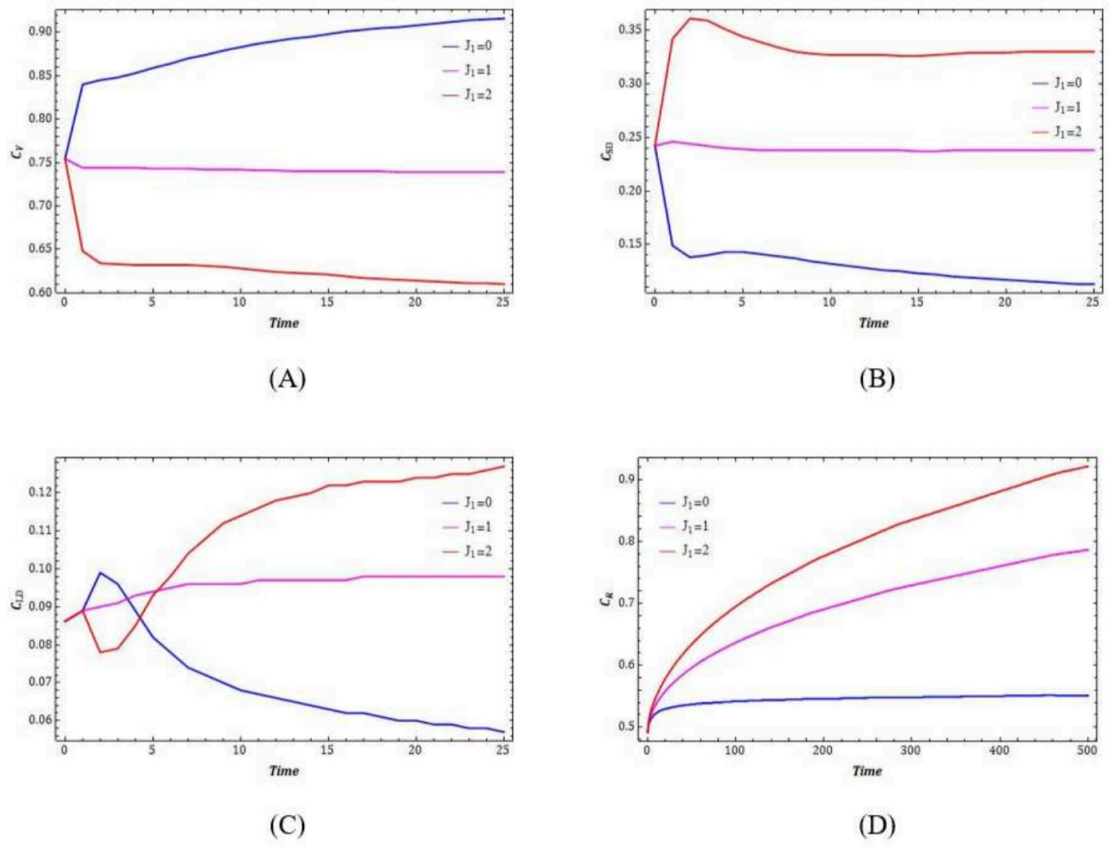

Figure 23: Variation in (A) C_V, (B) C_{SD}, (C) C_{LD} and (D) C_R for different values of J_1 and $\alpha = 0.5$

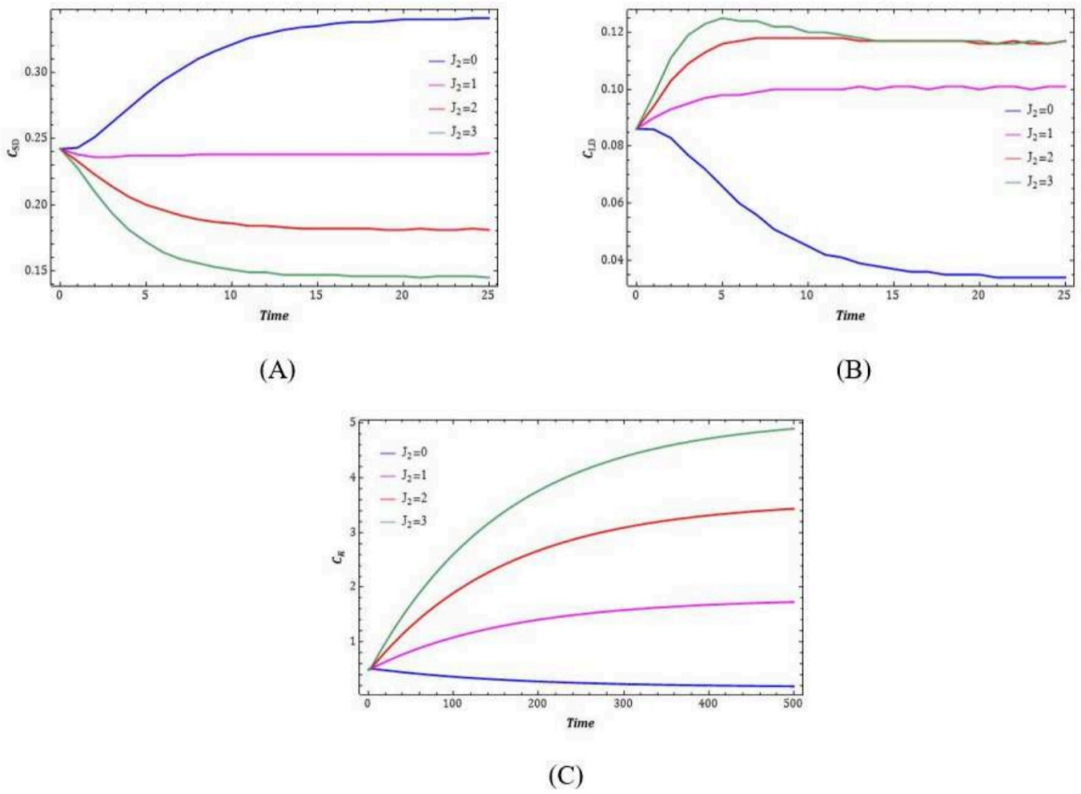

Figure 24: Variation in (A) C_V, (B) C_{SD}, (C) C_{LD} and (D) C_R for different values of J_2 and $\alpha = 1$

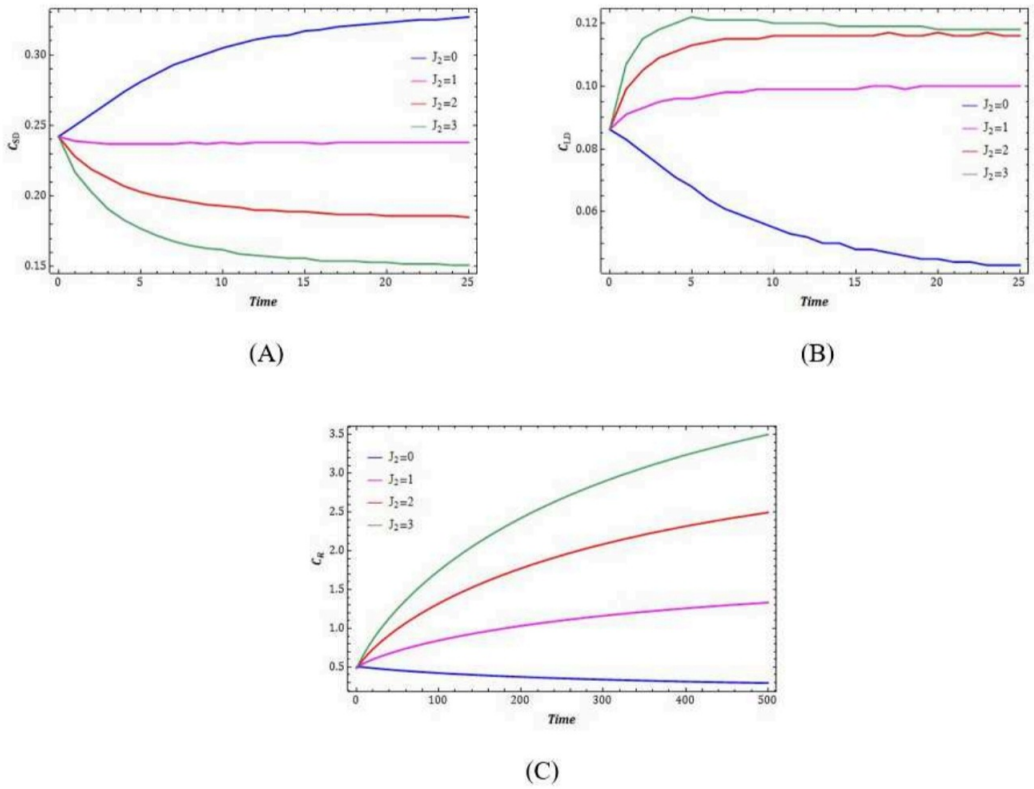

Figure 25: Variation in (A) C_{SD}, (B) C_{LD} and (C) C_R for different values of J_2 and $\alpha = 0.8$

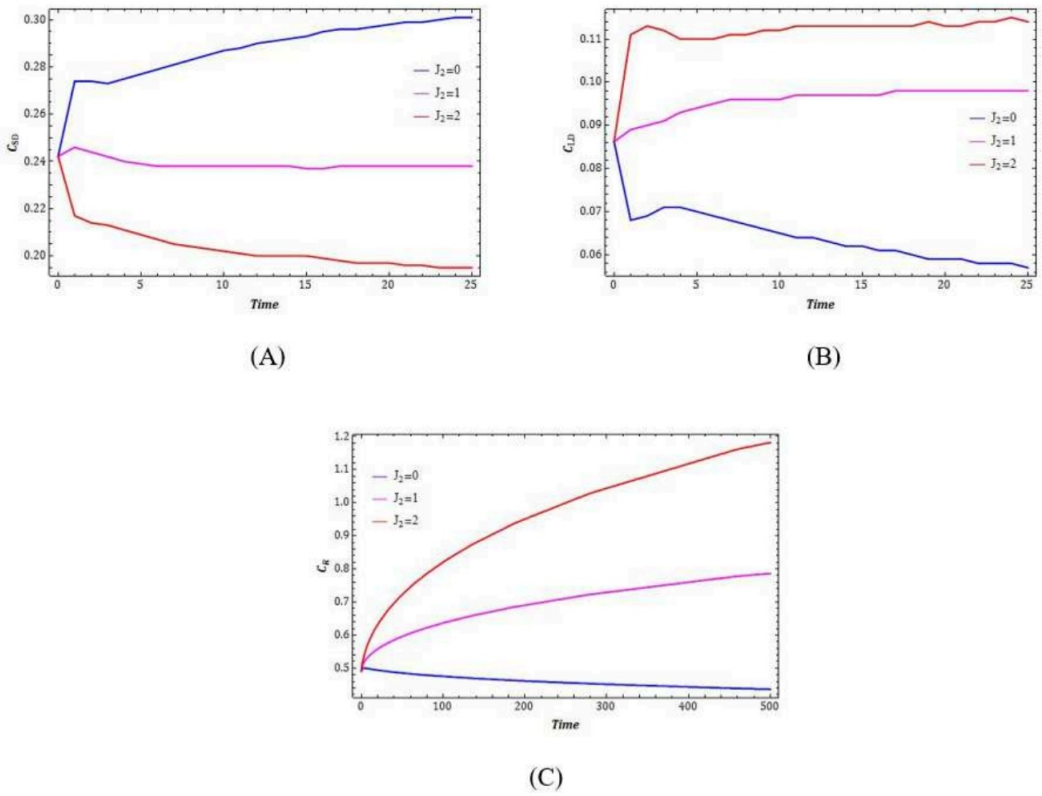

Figure 26: Variation in (A) C_{SD}, (B) C_{LD} and (C) C_R for different values of J_2 and $\alpha = 0.5$

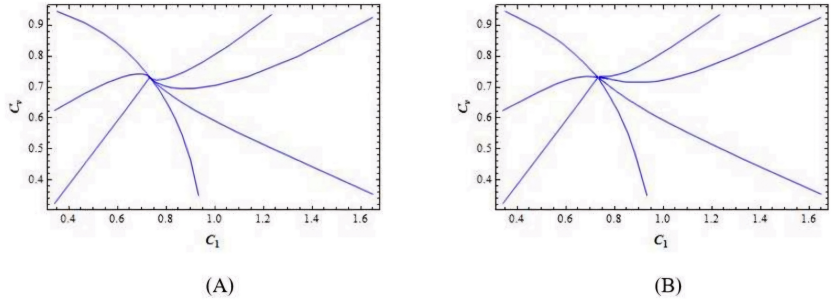

Figure 27: Global stability of (C_1, C_V) for (A) α=1 and (B) α=0.8.

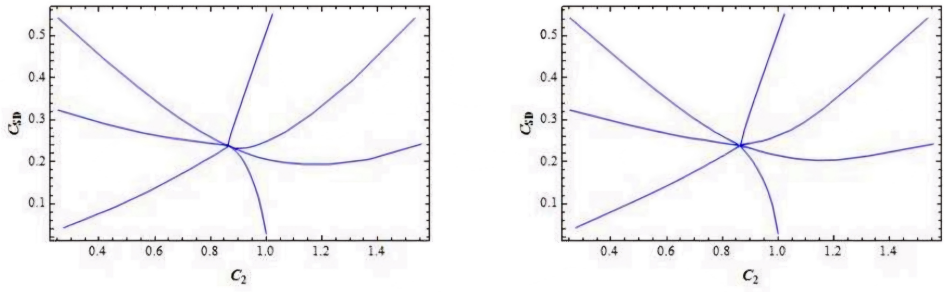

Figure 28: Global stability of (C_2, C_{SD}) for (A) α=1 and (B) α=0.8.

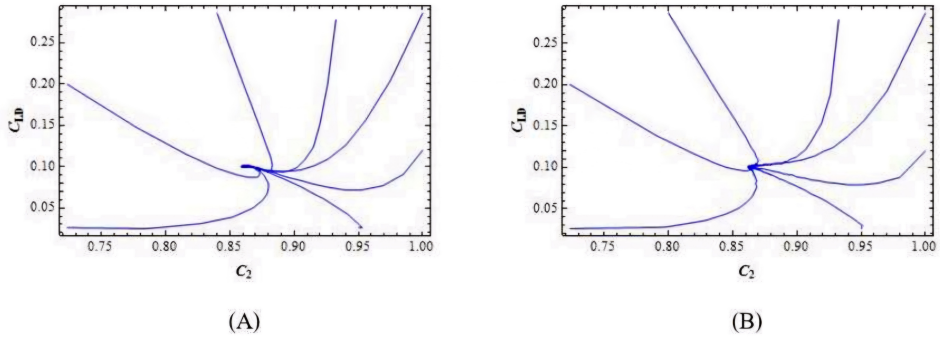

Figure 29: Global stability of (C_2, C_{LD}) for (A) α=1 and (B) α=0.8.

4.4 Conclusion

This study proposes a nonlinear math method for rainmaking using atmospheric particle introduction. The impact of fractional order derivative is examined through numerical analysis, confirming the effectiveness of the calculation in supporting the model's analytical outcomes. The model contends that rain formation necessitates a high concentration of water vapor in nature rather than ongoing production. To build up atmospheric water vapor molecules, continuous creation is required. The research suggests that increasing the aggregate concentration of beneficial aerosol particles boosts rainfall effectiveness. This new rainmaking model incorporates fractional derivatives and two types of aerosols for a more accurate depiction. The findings are convincing, correlating well with real-world processes and offering predictive utility.

References

[1] C. Xue, A. Friedman, and C. K. Sen, "A mathematical model of ischemic cutaneous wounds," *Proceedings of the National Academy of Sciences*, vol. 106, no. 39, pp. 16782–16787, 2009.

[2] B. P. Ingalls, *Mathematical modeling in systems biology: an introduction*. MIT press, 2013.

[3] J. D. Nagy, "The ecology and evolutionary biology of cancer: a review of mathematical models of necrosis and tumor cell diversity," *Mathematical Biosciences & Engineering*, vol. 2, no. 2, pp. 381–418, 2005.

[4] S. Bakshi, V. Chelliah, C. Chen, and P. H. van der Graaf, "Mathematical biology models of parkinson's disease," *CPT: pharmacometrics & systems pharmacology*, vol. 8, no. 2, pp. 77–86, 2019.

[5] B. Inan, M. S. Osman, T. Ak, and D. Baleanu, "Analytical and numerical solutions of mathematical biology models: The newell-whitehead-segel and allen-cahn equations," *Mathematical methods in the applied sciences*, vol. 43, no. 5, pp. 2588–2600, 2020.

[6] M. A. Nowak and R. M. May, "Mathematical biology of hiv infections: antigenic variation and diversity threshold," *Mathematical Biosciences*, vol. 106, no. 1, pp. 1–21, 1991.

[7] H. S. Rodrigues, "Application of sir epidemiological model: new trends," *arXiv preprint arXiv:1611.02565*, 2016.

[8] G. A. Dever, "An epidemiological model for health policy analysis," *Social indicators research*, vol. 2, pp. 453–466, 1976.

[9] M. Martcheva, *An introduction to mathematical epidemiology*, vol. 61. Springer, 2015.

[10] E. models: why and how to use them, "Ecological Models," 2024.

[11] D. J. Daley and J. M. Gani, *Epidemic modelling: an introduction*. No. 15, Cambridge university press, 1999.

[12] ScienceDirect, "Ecological Model," 2017.

[13] RHIhub, "Ecological Models," 2024.

[14] N. Schuwirth, F. Borgwardt, S. Domisch, M. Friedrichs, M. Kattwinkel, D. Kneis, M. Kuemmerlen, S. D. Langhans, J. Martínez-López, and P. Vermeiren, "How to make ecological models useful for environmental management," *Ecological Modelling*, vol. 411, p. 108784, 2019.

[15] L. J. Jackson, A. S. Trebitz, and K. L. Cottingham, "An introduction to the practice of ecological modeling," *BioScience*, vol. 50, no. 8, pp. 694–706, 2000.

[16] J. F. Sallis, N. Owen, E. Fisher, *et al.*, "Ecological models of health behavior," *Health behavior: Theory, research, and practice*, vol. 5, no. 43-64, 2015.

[17] R. Agarwal, S. Hristova, and D. O'Regan, "A survey of lyapunov functions, stability and impulsive caputo fractional differential equations," *Fractional Calculus and Applied Analysis*, vol. 19, no. 2, pp. 290–318, 2016.

[18] I. Podlubny, *Fractional differential equations: an introduction to fractional derivatives, fractional differential equations, to methods of their solution and some of their applications*. elsevier, 1998.

[19] T. Skovranek, I. Podlubny, I. Petras, and D. Bednarova, "Data fitting using solutions of differential equations: Fractional-order model versus integer-order model," in *Proceedings of the 13th International Carpathian Control Conference (ICCC)*, pp. 703–710, IEEE, 2012.

[20] N. J. Ford and A. C. Simpson, "The numerical solution of fractional differential equations: speed versus accuracy," *Numerical Algorithms*, vol. 26, pp. 333–346, 2001.

[21] M. Rahimy, "Applications of fractional differential equations," *Appl. Math. Sci*, vol. 4, no. 50, pp. 2453–2461, 2010.

[22] C. Baishya, S. J. Achar, and P. Veeresha, "An application of the caputo fractional domain in the analysis of a covid-19 mathematical model," *Contemporary Mathematics*, pp. 255–283, 2024.

[23] S. Achar and C. Baishya, "Mathematical analysis of pluviculture in the frame of caputo fractional derivative," *Indian Journal of Science and Technology*, vol. 14, no. 48, pp. 3509–3524, 2021.